Atmospheric
Chemistry
and Physics
Discussions

1 **Impact of air pollution control measures and regional transport on**

2 **carbonaceous aerosols in fine particulate matter in urban Beijing,**

3 **China: Insights gained from long-term measurement**

4 Dongsheng Ji[1, 2*], Wenkang Gao[1, 2], Willy Maenhaut[3*], Jun He[4], Zhe Wang[1, 5], Jiwei Li[1, 6], Wupeng

5 Du[7], Lili Wang[1, 2], Yang Sun[1, 2], Jinyuan Xin[1, 2], Bo Hu[1, 2], Yuesi Wang[1, 2*]

6 *[1] State Key Laboratory of Atmospheric Boundary Layer Physics and Atmospheric Chemistry,*

7 *Institute of Atmospheric Physics, Chinese Academy of Sciences, Beijing, 100191, China*

8 *[2] Atmosphere Sub-Center of Chinese Ecosystem Research Network, Institute of Atmospheric Physics,*

9 *Chinese Academy of Sciences, Beijing, 100191, China*

10 *[3] Department of Chemistry, Ghent University, Gent, 9000, Belgium*

11 *[4] Natural Resources and Environment Research Group, International Doctoral Innovation Centre,*

12 *Department of Chemical and Environmental Engineering, University of Nottingham Ningbo China,*

13 *Ningbo, 315100, China*

14 *[5] Research Institute for Applied Mechanics, Kyushu University, Fukuoka, 816-8580, Japan*

15 *[6] University of Chinese Academy of Sciences, Beijing, 100049, China*

16 *[7] Institute of Urban Meteorology, Chinese Academy of Meteorological Sciences, Beijing, 100081,*

17 *China*

18

19 Correspondence to: Dongsheng Ji (jds@mail.iap.ac.cn), Willy Maenhaut (Willy.Maenhaut@UGent.be)

20 and Yuesi Wang (wys@dq.cern.ac.cn)

Atmospheric
Chemistry
and Physics
Discussions

21   **Abstract** As major chemical components of airborne fine particulate matter ($PM_{2.5}$), organic carbon

22   (OC) and elemental carbon (EC) have vital impacts on air quality, climate change, and human health.

23   Because OC and EC are closely associated with fuel combustion, it is helpful for the scientific

24   community and policymakers assessing the efficacy of air pollution control measures to study on

25   the impact of the control measures and regional transport on the OC and EC levels. In this study,

26   hourly mass concentrations of OC and EC associated with $PM_{2.5}$ were semi-continuously measured

27   from March 2013 to February 2018. The results showed that annual mean OC and EC concentrations

28   declined from 14.0 to 7.7 $\mu g/m^3$ and from 4.0 to 2.6 $\mu g/m^3$, respectively, from March 2013 to

29   February 2018. In combination with the data of OC and EC in previous studies, an obvious

30   decreasing trend in OC and EC concentrations was found, which was caused by clean energy

31   policies and effective air pollution control measures. However, no obvious change in the ratios of

32   OC and EC to the $PM_{2.5}$ mass (on average, 0.164 and 0.049, respectively) was recorded, suggesting

33   that inorganic ions still contributed a lot to $PM_{2.5}$. Based on the seasonal variations of OC and EC,

34   it appeared that higher OC and EC concentrations were still observed in the winter months, with the

35   exception of winter of 2017-2018. Traffic policies executed in Beijing resulted in nighttime peaks

36   of OC and EC, caused by heavy-duty vehicles and heavy-duty diesel vehicles being permitted to

37   operate from 0:00 to 6:00. In addition, the fact that there was no traffic restriction in weekends led

38   to higher concentrations in weekends compared to weekdays. Significant correlations between OC

39   and EC were observed throughout the study period, suggesting that OC and EC originated from

40   common emission sources, such as exhaust of vehicles and fuel combustion. OC and EC levels

41   increased with enhanced SO_2, CO and NO_x concentrations while the O_3 and OC levels enhanced

42   simultaneously when O_3 concentrations were higher than 50 $\mu g/m^3$. Nonparametric wind regression

43   analysis was performed to examine the sources of OC and EC in the Beijing area. It was found that

44   there were distinct hot spots in the northeast wind sector at wind speeds of approximately 5 km/h,

45   as well as diffuse signals in the southwestern wind sectors, highlighting probable trans-boundary

46   transport from highly industrialized regions upwind of the Hebei province, such as Baoding,

47   Shijiazhuang and Handan, which were the most polluted cities in China. This was consistent with

48   their higher potential as source areas, as determined by the potential source contribution function

49   (PSCF) analysis. A high-potential source area was precisely pinpointed, which was located in the

50 northwestern and southern areas of Beijing in 2017 instead of solely in the southern areas of Beijing

51 in 2013. This work shows that improvement of the air quality in Beijing benefits from strict control

52 measures; however, joint prevention and control of regional air pollution in the regions is needed

53 for further improving the air quality. The results provide a reference for controlling air pollution

54 caused by rapid economic development in developing countries.

55

56 **Key words** air pollution control measures, regional transport, organic carbon, elemental carbon,
57 Beijing

Atmospheric
Chemistry
and Physics
Discussions

1 Introduction

Worldwide attention on atmospheric organic carbon (OC) and elemental carbon (EC) has been paid by the public and the scientific community because OC and EC have vital effects on air quality, atmospheric visibility, climate, and human health (Bond et al., 2013; Boucher et al., 2013; World Health Organization (WHO), 2012). OC is composed of thousands of organic compounds and occupies 10-50 % of the ambient $PM_{2.5}$ mass (Seinfeld and Pandis, 1998) while EC, which is emitted from fuel combustion, represents 1-13 % of the ambient $PM_{2.5}$ mass (Shah et al., 1986; Tao et al., 2017; Malm et al., 1994). Considering that OC and EC occupy high fractions of the $PM_{2.5}$, a decline in OC and EC concentrations will improve air quality. Due to the light scattering potential of OC and the light absorption ability of EC, high concentrations of OC and EC can impair the atmospheric visibility. In addition, OC and EC can affect the atmospheric energy balance through scattering and absorbing incoming and outgoing solar and terrestrial radiation (direct effect) and through modifying the microphysical properties of clouds, like influencing cloud condensation nuclei and/or ice nuclei (indirect effects). Direct and indirect effects of OC and EC remain one of the principal uncertainties in estimates of anthropogenic radiative forcing (Boucher et al., 2013). In particular, black carbon (BC also called EC) coated with secondary particles can enhance aerosol radiative forcing (Wang et al., 2013; Zhang et al., 2008). BC is found to aggravate haze pollution in megacities (Ding et al., 2016; Zhang et al., 2018). Most of all, OC and EC adversely affect human health. As important constituents of OC, polycyclic aromatic hydrocarbons (PAHs) are well known as carcinogens, mutagens, and teratogens and therefore pose a serious threat to the health and the well-being of humans (Boström et al., 2002). Short-term epidemiological studies provide sufficient evidence of all-cause and cardiovascular mortality and cardiopulmonary hospital admissions associated with daily variations in BC concentrations; besides, cohort studies proved that all-cause and cardiopulmonary mortality are linked with long-term average BC exposure (WHO, 2012). Thus, long-term continuous observations of OC and EC are a prerequisite to further study air quality, atmospheric visibility, climate effects, and human health. However, long-term continuous observations of OC and EC in China are scarce.

In the world, China is considered as one of the regions of high emissions of OC and EC due to high energy consumption and increasing vehicle population, accompanying rapid economic

87   development and urbanization for decades (http://www.stats.gov.cn/tjsj/ndsj/2017/indexch.htm). As

88   the capital of China, Beijing with a residential population of 21.7 million, domestic tourists of

89   2.9×10^2 million and foreign tourists of approximately 3.3 million in 2017

90   (http://tjj.beijing.gov.cn/English/AD/) faces severe air pollution problems, which have attracted

91   worldwide attention. A series of studies on OC and EC have already been performed in Beijing.

92   Lang et al. (2017) indicated that OC showed a downward trend and EC had almost no change before

93   2003, both increased from 2003 to 2007, but decreased after 2007. The decline in OC concentrations

94   was associated with coal combustion and motor vehicle emission control measures, while that in

95   EC was caused by the replacement of fossil fuel and control of biomass emissions. Tao et al. (2017)

96   stated that the nearly 30 % reduction in total carbon (TC) in recent years in Beijing can be taken as

97   a real trend. Lv et al. (2016) found that the concentrations of OC and EC remained unchanged from

98   2000 to 2010 in Beijing. Yang et al. (2011a) conducted a long-term study of carbonaceous aerosol

99   from 2005 to 2008 in urban Beijing and found a decline in the ratio of carbonaceous species to the

100    $PM_{2.5}$ mass in contrast to what was observed 10 years earlier, which indicated that the importance

101   of carbonaceous species in $PM_{2.5}$ had decreased. In addition, pronounced seasonal variations were

102   recorded with the highest concentrations occurring in winter and the lowest ones in summer. Overall,

103   these previous researches seem somewhat inconsistent with each other and they seldom focused on

104   studying the impact of air pollution control measures and regional transport on the carbonaceous

105   aerosol levels in detail.

106   Notably, a series of the strictest measures on emission abatement and pollution control were

107   implemented in China from September 2013 (Jin et al., 2016). Substantial manpower and material

108   resources have been put into improving the air quality in the past five years and significant measures

109   are being taken for the atmospheric environment and ecosystem (Gao et al., 2017). To evaluate the

110   effectiveness of air pollution control measures, it is necessary to conduct a long-term continuous

111   observation of OC and EC and to study their long-term variation. Most of the previous studies

112   showed average information for certain periods based on filter sampling and laboratory analysis and

113   did not reflect the dynamic evolution processes of OC and EC with hourly resolution, which can

114   provide important and detailed information for the potential health risk in the area with frequent

115   occurrence of air pollution episodes. In addition, long-term measurements in urban areas of China

Atmospheric
Chemistry
and Physics
Discussions

116   with high population density were scarce (Yang et al., 2005, 2011a; Zhang et al., 2011; Li et al.,

117   2015; Chang et al., 2017) and the knowledge on long-term continuous hourly observations is still

118   lacking, which is yet important for recognizing the influence of source emissions on air quality.

119   Based on the-above mentioned background, it is necessary to perform a long-term continuous

120   hourly observation to explore the characteristics of OC and EC, to examine the relationship between

121   OC and EC and with major air pollutants and their sources so as to better assess the influence of

122   emission control measures on the OC and EC levels. In this study, inter-annual, seasonal, weekly

123   and diurnal variation of OC and EC were investigated. The influence of local and regional

124   anthropogenic sources was evaluated using non-parametric wind regression (NWR) and potential

125   contribution source function (PSCF) methods. This study will be helpful for improving the

126   understanding of the variation and sources of OC and EC associated with $PM_{2.5}$ and assessing the

127   effectiveness of local and national PM control measures and it provides a valuable dataset for

128   atmospheric modelling study and assessing the health risk. It also is the first time that a continuous

129   hourly measurement for a 5-year period based on the thermal-optical method is reported for urban

130   Beijing.

131   **2 Experimental**

132   **2.1 Description of the site**

133   The study site (39°58'28'' N, 116°22'16'' E, 44 m above ground) was set up in the second floor

134   in the campus of the State key laboratory of atmospheric boundary physics and atmospheric

135   chemistry of the Institute of atmospheric Physics, Chinese Academy of Science (Fig. 1). The site is

136   approximately 1 km south from the 3rd Ring Road (main road), 1.2 km north from the 4th Ring

137   Road (main road), 200 m west of the G6 Highway (which runs north-south) and 50 m south of the

138   Beitucheng West Road (which runs east-west), respectively. The annual average vehicular speeds in

139   the morning and evening traffic peaks were approximately 27.8 and 24.6 km/h, respectively, in the

140   past five years. During the whole study period the level of traffic congestion is mild based on the

141   traffic   performance   index   published   by   the   Beijing   Traffic   Management   Bureau

142   (http://www.bjtrc.org.cn/), which indicated 1.5-1.8 times more time will be taken to publicly travel

143   during traffic peaks than during smooth traffic. The study site is surrounded by residential zones, a

144   street park and a building of ancient relics without industrial sources. The experimental campaign

Atmospheric
Chemistry
and Physics
Discussions

145   was performed from March 1, 2013 to February 28, 2018. The periods of March 1, 2013 to February

146   28, 2014, March 1, 2014 to February 28, 2015, March 1, 2015 to February 28, 2016, March 1, 2016

147   to February 28, 2017 and March 1, 2017 to February 28, 2018 are, hereinafter, called for short 2013,

148   2014, 2015, 2016 and 2017, respectively.

149   **2.2 Instrumentation**

150   Concentrations of $PM_{2.5}$-associated OC and EC were hourly measured with semi-continuous

151   thermal-optical transmittance method OC/EC analyzers (Model 4, Sunset Laboratory Inc. Oregon,

152   Unite states of America (USA)). The operation and maintenance are strictly executed according to

153   standard operating procedures (SOP, https://www3.epa.gov/ttnamti1/spesunset.html). Volatile

154   organic gases are removed by an inline parallel carbon denuder installed upstream of the analyzer.

155   A round 16-mm quartz filter is used to collect $PM_{2.5}$ with a sampling flow rate of 8 L/m. A modified

156   NIOSH thermal protocol (RT-Quartz) is used to measure OC and EC. The sampling period is 30

157   min and the analysis process lasts for 15 min. Calibration is performed according to the SOP. An

158   internal standard CH_4 mixture (5.0 %; ultra-high purity He) is automatically injected to calibrate the

159   analyzer at the end of every analysis. In addition, off-line calibration was conducted with an external

160   amount of sucrose standard (1.06 μg) every three months. The quartz fiber filters used for sample

161   collection were replaced by new ones before the laser correction factor dropped below 0.90. After

162   replacement, a blank measurement of the quartz fiber filters is carried out. The uncertainty of the

163   TC measurement has been estimated to be approximately ±20 % (Peltier et al., 2007). A US

164   Environmental Protection Agency Federal Equivalent Method analyzer of $PM_{2.5}$ (SHARP 5030,

165   Thermo-Fisher Scientific, Massachusetts, USA) was used to monitor $PM_{2.5}$ and ±5 % for 24 h is the

166   accuracy of the measurements. The operation, maintenance and calibration are strictly executed

167   according to the instruction manual of the Model SHARP 5030 $PM_{2.5}$ analyzer (Ji et al., 2016). The

168   data were processed using an Igor-based software (Wu et al., 2018) and the commercial software of

169   Origin.

170   **2.3 NWR and PSCF methods**

171   **2.3.1 NWR method**

172   NWR is a source-to-receptor source identification model, which provides a meaningful

173 allocation of local sources (Henry et al., 2009; Petit et al., 2017). Wind analysis results using NWR

174 were obtained using a new Igor-based tool, named ZeFir, which can perform a comprehensive

175 investigation of the geographical origins of the air pollutants (Petit et al., 2017). The principle of

176 NWR is to smooth the data over a fine grid so that concentrations of air pollutants of interest can be

177 estimated by any couple of wind direction (θ) and wind speed (u). The smoothing is based on a

178 weighing average where the weighing coefficients are determined using a weighting function $K(\theta,$

179 $u, \sigma, h) = K_1 (\theta, \sigma) \times K_2 (u, h)$ (i.e., Kernel functions). The estimated value (E) given θ and u is

180 calculated by the following equations (1)-(3):

181 $$E(\theta|u) = \frac{\sum_{i=1}^{N} K1\left(\frac{\theta - Wi}{\sigma}\right) \times K2\left(\frac{u - Yi}{h}\right) \times Ci}{\sum_{i=1}^{N} K1\left(\frac{\theta - Wi}{\sigma}\right) \times K2\left(\frac{u - Yi}{h}\right)} \qquad (1)$$

182 $$K_1(x) = \frac{1}{\sqrt{2\pi}} \times e^{-0.5x^2} \qquad -\infty < x < \infty \qquad (2)$$

183 $$K_2(x) = 0.75 \times (1 - x^2) \qquad -1 < x < 1 \qquad (3)$$

184 where σ and h were smoothing parameters, which can be suggested by clicking on the button of

185 suggest estimate in the software of Zefir; Ci, Wi, and Yi are the observed concentration of a pollutant

186 of interest, resultant wind speed and direction, respectively, for the ith observation in a time period

187 starting at time t_i; N is the total number of observations.

188   After the calculation, graphs of the estimated concentration and the joint probability are

189 generated. The NWR graph of the air pollutant of interest, acquired directly via the NWR calculation,

190 represents an integrated picture of the relationship of estimated concentration of the specific

191 pollutant, wind direction and wind speed. The graph of the joint probability for the wind data,

192 equivalent to a wind rose, shows the occurrence probability distribution of the wind speed and wind

193 direction.

194 **2.3.2 PSCF method**

195   The PSCF method is based on the residence time probability analysis of air pollutants of

196 interest (Ashbaugh et al., 1985). Source locations and preferred transport pathways can be identified

197 (Poirot and Wishinski, 1986; Polissar et al., 2001; Lupu and Maenhaut, 2002). The potential

198 locations of the emission sources are determined using backward trajectories. A detailed description

199 can be found in Wang et al. (2009). In principle, the PSCF is expressed using equation (4):

200 $$PSCF(i, j) = w_{ij} \times (m_{ij}/n_{ij}) \qquad (4)$$

Atmospheric
Chemistry
and Physics
Discussions

201   where w_{ij} is an empirical weight function proposed to reduce the uncertainty of n_{ij} during the study

202   period, m_{ij} is the total number of endpoints in (i, j) with concentration value at the receptor site

203   exceeding a specified threshold value and n_{ij} is the number of back-trajectory segment endpoints

204   that fall into the grid cell (i, j) over the period of study. In this study, the domain for the PSCF was

205   set in the range of (30-70 °N, 65-150 °E) with the grid cell size of $0.25 \times 0.25°$.

206   **3 Results and discussion**

207   **3.1 Levels of OC and EC**

208   Statistics for the OC and EC concentrations from March 1, 2013 to February 28, 2018 are

209   summarized in Table 1. Benefiting from the Air Pollution Prevention and Control Action Plan, a

210   decline in annual average concentrations is on the whole recorded. In detail, the annual average

211   concentrations of OC peaked in 2014 and then declined from 14.5 to 7.7 $\mu g/m^3$, whereas those of

212   EC also peaked in 2014 and then declined from 4.3 to 2.6 $\mu g/m^3$ during the study period. The decline

213   in OC and EC concentrations is closely associated with decreasing coal consumption, increasing

214   usage of natural gases and the implementation of a strict vehicular emission standard (Table 2).

215   Knowledge of the relative contribution of OC and EC to $PM_{2.5}$ is important in formulating effective

216   control measures for ambient PM (Wang et al., 2016a). The ratios of OC and EC to $PM_{2.5}$ varied

217   little during the whole study period. The ratios of OC to $PM_{2.5}$ ranged from 15.5 to 17.8 % with the

218   average of 16.4 %, while those of EC to $PM_{2.5}$ ranged from 4.5 to 5.2 % with the average of 4.9 %.

219   OC accounted, on average, for 77.0 ± 9.3 % of the total carbon (TC, the sum of OC and EC), while

220   EC amounted for 23.0 ± 9.3 % of the TC. These results are consistent with those in previous studies

221   (Wang et al., 2016a; Tao et al., 2017, Lang et al., 2017). The contribution of TC to $PM_{2.5}$, $21.3 \pm$

222   15.8 %, is also similar to those reported in previous studies, listed in Table S1, for example, at urban

223   sites of Hongkong, China (23.5-23.6 % in 2013), Hasselt (23 %) and Mechelen (24 %) in northern

224   Belgium, rural sites in Europe (19-20 %) and some sites in India (on average, 20 %, Bisht et al.,

225   2015; Ram and Sarin, 2010; Ram and Sarin, 2012), but lower than those observed historically at

226   multiple sites in China (on average 27 %, Wang et al., 2016a), with Beijing (27.6 %, from March

227   2005 to Feb 2006), Chongqing (28.3 %, from March 2005 to February 2006), Shanghai (34.5 %,

228   from March 1999 to May 2000) and Guangzhou (26.4 %, December 2008 to February 2009), in

229   Budapest (40 %), Istanbul (30 %), and many sites in the USA, like Fresno (43.2 %), Los Angeles

Atmospheric
Chemistry
and Physics
Discussions

230   (36.9 %) and Philadelphia (33.3 %) (Na et al., 2004). Compared to previous studies, the ratio of TC

231   to PM$_{2.5}$ became smaller, indicating a smaller contribution of carbonaceous aerosols to PM$_{2.5}$. A

232   higher ratio of TC to PM$_{2.5}$ suggests that there is a lower contribution from secondary inorganic ions

233   to PM$_{2.5}$, while a lower ratio may indicate a larger contribution from secondary inorganic ions to

234   PM$_{2.5}$. The carbonaceous aerosol (the sum of multiplying the measured OC by a factor of 1.4 and

235   EC) represented on average, 27.7 ± 16.7 % of the observed PM$_{2.5}$ concentration, making it a

236   dominant contributor to PM$_{2.5}$.

237   Table 2 lists recently published results for OC and EC mass concentrations in major megacities.

238   Although the observation periods were not same, a comparative analysis of OC and EC

239   concentrations between different megacities could show the status of energy consumption for

240   policymakers, drawing lessons and experience from other countries. It is obvious that the PM$_{2.5}$-

241   associated OC and EC levels in the megacities in the developing countries were far higher than

242   those in the developed countries. The PM$_{2.5}$-associated OC and EC concentrations in Beijing were

243   higher than those in Athens, Greece (2.1 and 0.54 μg/m^3), Los Angeles (2.88 and 0.56 μg/m^3) and

244   New York (2.88 and 0.63 μg/m^3), USA, Paris, France (3.0 and 1.4 μg/m^3), Soul, South Korea (4.1

245   and 1.6 μg/m^3), Tokyo, Japan (2.2 and 0.6 μg/m^3) and Toronto, Canada (3.39 and 0.5 μg/m^3). That

246   is because clean energy has widely been used and strict control measures are taken to improve the

247   air quality step by step in the developed countries. Of the megacities in the developing countries,

248   OC and EC concentrations in Beijing were lower than those in most other megacities, like Mumbai

249   and New Delhi, India, and Xi'an and Tianjin, China, but close to those in Shanghai and Hongkong,

250   China, and higher than those in Lhasa, China. These differences/similarities indicate that OC and

251   EC gradually declined in Beijing and that a series of measures had progressive effects. However, to

252   further improve the air quality, more synergetic air pollution abatement measures of carbonaceous

253   aerosols and volatile organic compounds (VOCs) emissions need to be performed.

254   Fig. 2 shows the mass fractions of carbonaceous aerosols in different PM$_{2.5}$ levels classified

255   according to PM$_{2.5}$ concentrations during the whole study period. There were 571, 561, 310, 169,

256   142 and 74 days for excellent, good, slightly polluted, moderately polluted, heavily polluted and

257   severely polluted air quality levels during the whole period. It was obvious that OC and EC

258   concentrations increased with the degradation of air quality. OC and EC concentrations were 6.3

Atmospheric
Chemistry
and Physics
Discussions

259   and 1.7, 10.2 and 2.9, 13.7 and 4.1, 17.3 and 5.3, 24.6 and 7.9 and 35.5 and 11.3 μg/m^3 for excellent,

260   good, slightly polluted (LP), moderately polluted (MP), heavily polluted (HP) and severely polluted

261   (SP) air quality days, respectively. However, the percentages of OC and EC accounting to PM$_{2.5}$

262   decreased with the deterioration of air quality. OC and EC made up for 31.5 % and 8.3 %, 18.9 %

263   and 5.4 %, 14.7 % and 4.4 %, 13.4 % and 4.1 %, 12.9 % and 4.2 % and 11.4 % and 3.6 % during

264   excellent, good, slightly polluted, moderately polluted, heavily polluted and severely polluted air

265   quality days, respectively. The percentage for OC decrease from 31.4 to 11.4 % while that for EC

266   decreased from 8.3 to 3.6 % with the deterioration of air quality, indicating that other PM$_{2.5}$

267   constituents than OC and EC contributed more to the increased PM$_{2.5}$ levels. This is consistent with

268   previous studies showing that secondary inorganic ions play a more important role in the increase

269   in PM$_{2.5}$ concentrations (Ji et al., 2014, 2018).

270   **3.2 Inter-annual variation of OC and EC**

271   To evaluate the effect of the clean air act over a prolonged period, our OC and EC data were

272   combined with the data of previous studies for Beijing. As shown in Figs. 3 and 4, a decreasing

273   trend in OC and EC concentrations is on the whole observed. The decline in OC and EC

274   concentrations was closely associated with a combined effect of stricter standards for vehicle

275   emissions, the increase in usage of natural gases and electricity consumption and the decreasing

276   consumption of coal and diesel oil, although the gross domestic product, population, energy

277   consumption and vehicular population rapidly increased (Table 2). In particular, there is an obvious

278   dividing line of OC and EC concentrations in 2010. After 2010, the OC and EC concentrations were

279   lower than those observed previously. This is because that Shougang Corporation, which is one of

280   the China's largest steel companies, moved out of Beijing and highly polluted factories on the

281   Beijing   outskirts   relocated   in   2010   (http://www.china.org.cn/business/2011-

282   01/13/content_21731198.htm) in addition to the gradual reduction of coal consumption and

283   increasing usage of clean energy like natural gases and electricity. In addition, all the small coal

284   mines in Beijing shut down and plenty of yellow label (heavy-polluting) vehicles were forced off

285   road. It resulted in an obvious decline in OC and EC concentrations from 2011. Note that the OC

286   and EC levels in 2008 and 2009 were also somewhat lower, which was caused by a series of

287   measures to improve the air quality for the Olympic Games in 2008 and a decline in industrial

Atmospheric
Chemistry
and Physics
Discussions

Open Access

288 production because of China's exports crash in 2009, respectively. It suggests that a stringent clean

289 air act and rectifying industry played important roles in the air quality improvement.

290   Similar to OC and EC, the annual mean SO_2 and NO_2 concentrations also showed a decreasing

291 trend. As well-known, SO_2 originates from coal combustion and the usage of sulfur-containing oil

292 (Seinfeld and Pandis, 1998). With the replacement of coal combustion for industrial production,

293 residential heating and cooking by clean energy (e.g., natural gases, electricity and lower sulfur

294 content in oil), a clear decline in annual SO_2 concentrations was observed in the Beijing area starting

295 from 2002. Compared with SO_2, OC and EC came from vehicular emission and biomass burning

296 besides coal combustion. Thus, the decline in coal consumption only played a partial role in the

297 decrease in the annual mean OC and EC concentrations. The rapid increase of vehicle population

298 partly offset the great effort in eliminating coal consumption, although standards for vehicle

299 emissions were also raised. As important products of vehicular emission, OC and EC did not decline

300 as SO_2. Similar to NO_2, which comes from the direct emission of vehicles or the oxidation of NO

301 from vehicular exhaust, OC and EC declined gradually but at a lower rate. It suggests that further

302 control of vehicular emissions will be useful to lower the OC and EC concentrations. Note also that

303 the effective control of biomass burning contributed a lot to the decrease in OC and EC

304 concentrations. As shown in Fig. 3, the decline in the number of fire spots was somehow correlated

305 with decreasing OC and EC concentrations in the past five years.

306 **3.3 Monthly and seasonal variations**

307   Fig. S1 shows the monthly mean OC and EC concentrations at our study site for the whole 5-

308 year period. Similar variations are observed with generally higher mean OC and EC levels in the

309 colder months (from November to February) and lower ones in the warm months (from May to

310 October). The highest average OC and EC concentrations were 24.1 ± 18.7 μg/m^3 in December 2016

311 and 9.3 ± 8.5 μg/m^3 in December 2015, respectively. However, the lowest OC and EC levels were

312 not observed in the warm months; they were 5.0 ± 4.6 μg/m^3 in January, 2018 and 1.5 ± 1.7 μg/m^3

313 in December, 2017, respectively; this was associated with both frequent occurrence of cold air mass

314 and the implementation of a winter radical action plan in Beijing from November, 2017. Overall,

315 the increased fuel consumption for domestic heating in addition to unfavorable meteorological

316 conditions in the colder months is considered to lead to higher OC and EC levels (Ji et al., 2014).

Atmospheric
Chemistry
and Physics
Discussions

317   In the warm months no energy is consumed for domestic heating and the wet scavenging by frequent

318   precipitation occurring in these months gives rise to lower OC and EC levels. In the warm months,

319   the monthly mean OC and EC concentrations decreased almost year by year. In contrast, in the cold

320   months no decline in the monthly mean OC and EC concentrations could be seen. The interquartile

321   ranges of OC and EC in the warm months was narrower than those in cold months, indicating that

322   there was more substantial variation in concentration in these months. The larger variation in the

323   colder months was caused by the cyclic accumulation and scavenging processes (Ji et al., 2012).

324   The successive accumulation processes were closely associated with unfavorable meteorological

325   conditions, which gave rise to higher OC and EC concentrations, while scavenging processes by

326   cold fronts led to lower levels.

327   As to the seasonality in OC and EC, similar seasonal variations are observed in the various

328   years with generally higher mean concentrations in autumn and winter and lower levels in spring

329   and summer (Fig. 5). The seasonal variations are explained by both changes in emission strength

330   and in meteorology (Cao et al., 2007). The high concentrations in winter are thought to be mainly

331   associated with emission from residential heating (biomass burning for heating occasionally

332   occurred in autumn and winter although biomass burning has been prohibited by the national laws,

333   regulations and policies.) along with unfavorable meteorological conditions such as lower mixing

334   layer height, temperature inversion, calm wind leading to less pollutant transport and a higher

335   relative humidity promoting secondary conversion of air pollutants (Ji et al., 2014, Zheng et al.,

336   2015). In addition, the lower air temperature in winter led to shifting the gas-particle equilibrium of

337   semi-volatile organic compounds (SVOCs) into the particle phase, resulting in the higher OC levels.

338   In autumn and winter, the cold start of vehicles (5.64 million vehicles in Beijing at the end of 2017)

339   also increased the emission of OC. On the other hand, the higher planetary boundary layer (PBL)

340   and larger wind speeds in spring and summer led to higher ventilation and more dispersion of

341   pollutants. In spring and summer, the higher temperature shifted the gas-particle equilibrium of

342   semi-volatile organic compounds towards the gas phase. In addition, OC and OC can also be

343   effectively scavenged by frequent precipitation in summer.

344   Remarkably, the OC and EC concentrations in the autumn and winter of 2017 were lower than

345   those in the previous years. This was due to the combined effect of controlling anthropogenic

Atmospheric
Chemistry
and Physics
Discussions

346   emissions strictly and the favorable meteorological conditions. Since September 2017, a series of

347   the most stringent measures within the Action Plan on Prevention and Control of Air Pollution were

348   implemented to improve the air quality; these measures included restricting industrial production

349   by shutting down thousands of polluting plants, suspending the work of iron and steel plants in 28

350   major cities and limiting the use of vehicles and reducing coal consumption as a heating source in

351   northern China. In addition, the air quality improvement in the autumn and winter of 2017 was

352   closely tied to frequent cold fronts accompanied by strong winds, which was favorable for

353   dispersing the pollutants. The average OC and EC concentrations in the winter were 1.69 and 1.14,

354   2.17 and 1.93, 1.49 and 2.14, 2.41 and 2.29 and 0.80 and 0.88 times higher than those in the summer

355   for 2013, 2014, 2015, 2016 and 2017, respectively. The difference in the ratios for 2017 was due to

356   the series of the most stringent measures taking effect and the favorable meteorology. The Beijing

357   municipal government in particular has made great efforts to replace coal by natural gases and

358   electricity-powered facilities. Besides, new energy vehicles are increasingly used to replace the

359   gasoline vehicles.

360   **3.4 Diurnal variation and weekly pattern for OC and EC**

361   As can be seen in Figs. S2 and S3, a clear diurnal variation is observed for both OC and EC in

362   each year. This variation is closely tied to the combined effect of diurnal variation in emission

363   strength and evolution of the PBL. The pattern for EC with higher concentrations in the nighttime

364   (from 20:00 to 4:00) and lower levels in the daytime (from 9:00 to 16:00) is largely linked to the

365   vehicular emissions. The EC concentrations increased starting from 17:00, corresponding with the

366   evening rush hours, emission from nighttime heavy-duty diesel trucks (HDDT) and heavy-duty

367   vehicles (HDV) and the formation of a nocturnal stable PBL. As regulated by the Beijing Traffic

368   management Bureau (http://www.bjjtgl.gov.cn/zhuanti/10weihao/), HDV and HDDT are allowed to

369   enter the urban area inside the 5th Ring Road from 0:00 to 06:00 (local Time). At other times, both

370   the higher PBL height and lower traffic intensity resulted in lower EC concentrations. The amplitude

371   of the diurnal variation in the EC concentrations was smaller in the last three years. The maximum

372   peak concentration (22:00-7:00) was 1.68, 1.62, 1.43, 1.40 and 1.40 times higher than that observed

373   in the valley period (13:00-15:00) for 2013, 2014, 2015, 2016 and 2017, respectively. Similar to EC,

374   the diurnal pattern for OC was also characterized by concentrations in the nighttime (from 20:00 to

375 4:00) and lower levels in the daytime (from 14:00 to 16:00). However, the formation of secondary

376 organic carbon from gas-phase oxidation of VOCs with increased solar radiation during midday

377 gave rise to a small additional peak of OC. Like for EC, the amplitude of the diurnal variation in the

378 OC concentrations was smaller in the last three years. The maximum peak concentration (19:00-

379 3:00) was 1.47, 1.47, 1.30, 1.34 and 1.26 times higher than that observed in the valley period (14:00-

380 16:00) for 2013, 2014, 2015, 2016 and 2017, respectively. Separate diurnal variations of OC and

381 EC for each season in each year are shown in Figs S4 and S5. Similar patterns are observed in in

382 the four seasons but the difference between peak and valley levels is larger in the winter than in the

383 other three seasons. The larger variation in the winter is due to the additional emission from

384 residential heating and more unfavorable meteorological conditions (Ji et al., 2016).

385   The difference in diurnal pattern between weekdays and weekends was also examined, see Figs.

386 S6 and S7. Similar diurnal variations are found on weekdays and weekend days. The maximum

387 peak concentration for EC (22:00-7:00) was 1.55, 1.43, 1.55, 1.51, 1.51, 1.46 and 1.59 times higher

388 than the valley concentration (13:00-15:00) for Monday, Tuesday, Wednesday, Thursday, Friday,

389 Saturday and Sunday, respectively, while the maximum peak concentration for OC (19:00-3:00)

390 was 1.41, 1.32, 1.38, 1.43, 1.37, 1.31 and 1.43 times higher than the valley concentration (14:00-

391 16:00) for Monday, Tuesday, Wednesday, Thursday, Friday, Saturday and Sunday, respectively. In

392 contrast to previous studies (Grivas et al., 2012; Jeong et al., 2017; Chang et al., 2017), OC and EC

393 exhibited higher concentrations on weekends than on weekdays. The average OC and EC

394 concentrations on Saturday and Sunday were 13.2 ± 1.8 $\mu g/m^3$ and 3.9 ± 2.7 $\mu g/m^3$ and 12.0 ± 10.4

395 $\mu g/m^3$ and 3.7 ± 3.6 $\mu g/m^3$, respectively, whereas the average OC and EC levels during the weekdays

396 were 11.8 ± 1.8 $\mu g/m^3$ and 3.6 ± 3.5 $\mu g/m^3$, respectively. This indicates that there is no significant

397 decline in anthropogenic activity in the weekends compared to weekdays. In fact, enhanced

398 anthropogenic emissions could be caused by no limit on driving vehicles based on license plate on

399 weekends. The larger OC and EC concentrations in the weekend are thus mainly attributed to

400 enhanced traffic emissions, which is consistent with higher NO_2 and CO concentrations in the

401 weekend (on average 56.6 ± 35.9 $\mu g/m^3$ for NO_2 and 1.16 ± 1.18 mg/m^3 for CO on weekdays

402 (number of samples = 29492); 57.8 ± 37.0 $\mu g/m^3$ for NO_2 and 1.25 ± 1.18 mg/m^3 for CO on

403 weekends (number of samples = 11881)).

Atmospheric
Chemistry
and Physics
Discussions

Open Access

3.5 Relationship between OC and EC and with gaseous pollutants

404

405　　　The relationship between particulate OC and EC is an important indicator that can give

406　　information on the origin and chemical transformation of carbonaceous aerosols (Chow et al., 1996).

407　　Fig. 6 presents the regression between the OC and EC concentrations for the $PM_{2.5}$ samples of the

408　　separate years 2013 to 2017. Significant correlations (R^2 ranging from 0.87 to 0.66) were observed

409　　with the slopes declining from 3.6 to 2.9 throughout the study period. The significant correlations

410　　suggest that in most cases OC and EC originated from similar primary sources. The slopes are

411　　consistent with the OC/EC ratios ranging from 2.0 to 4.0 for urban Beijing in previous studies (He

412　　et al., 2001; Dan et al., 2004; Zhao et al., 2013; Ji et al., 2016). In addition, the average OC/EC

413　　ratios observed in this study are comparable to those observed at other urban sites with vehicular

414　　emission as a dominant source in China and foreign countries, but lower than those in cities where

415　　coal is an important source of the energy needed (Table 4). The decline in the OC/EC ratio may be

416　　caused by decline in coal consumption and restriction in biomass burning. Coal combustion,

417　　biomass burning and secondary formation give rise to higher OC/EC ratios while vehicular emission

418　　result in lower ones (Cao et al., 2005).

419　　　EC and part of the OC originate from primary anthropogenic emissions, including fossil fuel

420　　combustion and biomass burning (Bond et al., 2013), and secondary OC is formed along with ozone

421　　formation. Hence, long-term and concurrent measurement of OC, EC, SO_2, NO_x, CO and O_3 is

422　　helpful for understanding the emission features or formation processes and for providing tests to

423　　current emission inventories. The variation in the OC and EC as a function of the SO_2, NO_x, CO

424　　and O_3 concentration is shown in Fig. 7. There is a clear increase in OC and EC with increasing

425　　SO_2, NO_x and CO, suggesting that the latter played a role in the enhancement of the former and that

426　　these various species shared common sources although they have a different lifetime. OC and EC

427　　increased, on average, by approximately 8.9 μg/m^3 and 5.7 μg/m^3, respectively, with an increase of

428　　2 mg/m^3 in CO. Considering that CO has a long lifetime (Liang et al., 2004) and that its increase

429　　depends on source strength and meteorology, high CO concentrations usually occur in the heating

430　　season when unfavorable meteorological conditions prevail. At very high CO concentrations, the

431　　increase in OC becomes slower than that in EC. This can be explained by that local emissions

432　　became dominant because the unfavorable meteorological conditions corresponding with the high

433   CO concentrations resulted in a weak exchange of air on the regional scale. The OC/EC ratio

434   declined at very high CO concentrations. This could be because vehicular emissions became the

435   dominant pollution source and gradually replaced the industrial emissions in Beijing

436   (http://language.chinadaily.com.cn/2018-05/15/content_36203449.htm).   As   documented   by

437   previous studies (Schauer et al., 2002, Na et al., 2004), emission of gasoline vehicles results in an

438   OC/EC ratio varying from 3 to 5 while that of diesel vehicles is below 1. The above results are

439   consistent with previous studies which showed that gasoline and diesel vehicles give rise to higher

440   CO emissions (Wu et al., 2016).

441   Given that NO_x and CO have some common emission sources (Hassler et al., 2016), the OC

442   and EC levels were also analyzed in different intervals of NO_x concentrations. Both OC and EC are

443   enhanced with increasing NO_x concentrations. Their enhancements were 5.0 μg/m^3 and 2.1 μg/m^3,

444   respectively, for an increase in NO_x concentration of 40 μg/m^3. Although NO_x are highly reactive

445   and have a short lifetime (Seinfeld and Pandis, 1998) in contrast to CO, the OC/EC ratio also

446   declined at very high NO_x concentrations, be it to a lesser extent than was the case at very high CO

447   concentrations. As was the case for high CO concentrations, more stable meteorological conditions

448   and local emissions became prevailed when higher concentrations of NO_x were observed. In fact,

449   63.5 % of all NO_x emissions comes from vehicular emissions based on the statistical data of air

450   pollutant   emissions   in   Beijing

451   (http://www.bjepb.gov.cn/bjhrb/xxgk/ywdt/zlkz/hjtj37/827051/index.html).

452   Examining the variation of OC and EC for different intervals of SO_2 concentrations allows us

453   to further study the impacts of industrial production or coal combustion on the OC and EC levels.

454   Similar to the relationship between CO and the carbonaceous species, the OC and EC concentrations

455   enhanced with increasing SO_2 concentrations. Their enhancements were 2.8 μg/m^3 and 0.7 μg/m^3,

456   respectively, for an increase in SO_2 concentration of 10 μg/m^3. An increase in the OC/EC ratio

457   occurred at large SO_2 concentrations, suggesting that coal consumption provided a substantial

458   contribution to the OC and EC levels in Beijing. Because oil with a low sulfur content has been

459   widely used in Beijing since 2008 and little coal was used in the urban areas of Beijing, the SO_2

460   mostly originated from industrial production in the surrounding areas of Beijing and from coal

461   combustion for residential heating in the suburban and rural areas of Beijing. Previous studies also

Atmospheric
Chemistry
and Physics
Discussions

462   showed that a higher OC/EC ratio is due to coal consumption and not from vehicular emissions

463   (Cao et al., 2005). Hence, coal combustion (for industrial production) on the regional scale led to

464   the enhancement of both the OC/EC ratio and SO_2 concentrations in Beijing via long-range transport.

465   Emissions of primary air pollutants lead to the formation of ozone and secondary organic

466   carbon (SOC) through multiple pathways (Seinfeld and Pandis, 1998), both of which are the

467   principal components of photochemical smog. Thus, the relationship of OC and O_3 is helpful for

468   understanding the variation and formation of OC and O_3. The OC concentrations were highest for

469   an O_3 concentration of 50 $\mu g/m^3$, which is approximately the average O_3 concentration in Beijing

470   in winter (Cheng et al., 2018). For O_3 concentrations above 100 $\mu g/m^3$, the O_3 and OC concentrations

471   enhanced simultaneously. This was because that the increased O_3 formation in favorable

472   meteorological conditions enhanced atmospheric oxidation and thereby the generation of SOC. This

473   gave rise to a concurrent increase in O_3 and OC concentrations. However, OC declined for O_3

474   concentrations increasing from 50 to 100 $\mu g/m^3$. Lower O_3 concentrations were observed when

475   unfavorable meteorological conditions or scavenge processes occurred. Usually lower O_3

476   concentrations accompanying lower OC concentrations are caused by scavenging processes such as

477   rainfall and strong winds. However, the unfavorable meteorological conditions led to the loss of O_3

478   via titration of NO trapping in the lower mixed layer height and accumulation and conversion of

479   OC. In addition, scattering and absorbing effects of aerosols that were trapped in lower mixed layer

480   led to less solar radiation reaching the ground and further restrained the O_3 formation (Xing et al.,

481   2017; Wang et al., 2016b).

482   **3.6 Impact of atmospheric transport on the OC and EC concentrations**

483   Figs. 8 and 9 show the results of the NWR analysis applied to 1-h $PM_{2.5}$-associated OC and

484   EC concentrations measured from 2013 and 2017 in Beijing. Fig. S8 presents the gridded emissions

485   of OC and BC for the Beijing-Tianjin-Hebei (BTH) region and China, based on emission inventory

486   (Zheng et al., 2018). The NWR results exhibit distinct hot spots (higher concentrations) in the

487   northeast wind sector at wind speeds of approximately 0-6 km/h, which were closely associated

488   with local emissions under stagnant meteorological conditions (low wind speed), as well as diffuse

489   signals in the southwestern wind sector, highlighting probable trans-boundary transport from highly

490   industrialized regions upwind of the Hebei province of China, such as Baoding, Shijiazhuang and

Atmospheric
Chemistry
and Physics
Discussions

491   Handan, which were the most polluted cities in China. Previous studies found high loadings of OC

492   and EC in Baoding, Shijiazhuang and Handan (http://english.mee.gov.cn/Resources/Reports/soe/).

493   The joint probability data in Figs. 14 and 15 show prevailing winds were from N to E and from S

494   to W with wind speeds of approximately 1-6 km/h and of approximately 4-9 km/h, respectively.

495   Note further that the hot spots of OC are broader than those of EC in the graphs of estimated

496   concentrations; this might be due to the fact that the VOCs (the precursors of SOC) emitted from

497   upwind areas, including the SW wind sector, led to an increase in OC concentrations at the receptor

498   site during the atmospheric transport while the EC concentrations slowly declined due to dilution

499   and deposition during the atmospheric transport.

500   Considering that the NWR analysis can only provide an allocation of local sources, the PSCF

501   analysis is a helpful complement to investigate potential advection of pollution over larger

502   geographical scales. Fig. 10 presents the PSCF results for OC and EC for the years 2013 to 2017.

503   Similar to the NWR analysis, the PSCF results indicated that local emissions and regional transport

504   from southerly areas were important contributors to the OC and EC loadings during the whole study

505   period. Only slight differences in the potential source regions are observed between the different

506   years. In 2013, a clear high potential source area was recorded for both OC and EC; it was located

507   in the southern plain areas of Beijing, particularly in the adjacent areas of the Hebei, Henan,

508   Shandong, Anhui and Jiangsu provinces. This was because there were intensified anthropogenic

509   emissions from those in 2013. The high pollutant emissions were caused by rapid economic growth,

510   urbanization and increase in vehicle population, energy consumption and industrial activity in the

511   southern plain areas of Beijing (Zhu et al., 2018), which resulted in a high aerosol loading in the

512   downwind areas. This result is consistent with previous studies (Ren et al., 2004; Wu et al., 2014; Ji

513   et al., 2018). In contrast to 2013, in the years 2014 to 2017 the high potential source regions for OC

514   and EC stretched to the juncture of Inner Mongolia and the Shaanxi and Shanxi provinces, and even

515   to the juncture of Inner Mongolia and the Ningxia Hui Autonomous Region and of Inner Mongolia

516   and the Gansu province. This is consistent with coal power plants being abundant in the above areas

517   (Liu F. et al., 2015). As well known, coal power plants are also important emitters of SO_2, and those

518   emissions were seen in satellite images (Li et al., 2017; Zhang et al., 2017), thus proving evidence

519   for those sources. The potential source areas for OC and EC were similar in 2013 and 2014. Overall,

520 the potential source areas were more intense for OC than for EC. The emission of OC precursors

521 (i.e., volatile organic compounds) from the Hebei, Henan, Shandong, Anhui, Jiangsu, Shanxi and

522 Shaanxi provinces led to OC concentrations downwind via chemical conversion during the

523 atmospheric transport. The widest potential source areas for OC and EC were recorded in 2016 and

524 they expanded into the eastern areas of Xinjiang Uyghur Autonomous Region. They are probably

525 associated with the economic boom in the western areas of China. In 2015, the potential source

526 areas were like in 2013 and 2014 also more intense for OC than for EC. Although the winter action

527 plan was enforced in Beijing, Tianjin and 26 surrounding cities (the so-called "2+26 cities"),

528 whereby the industrial output was curtailed, inspections of polluting factories were ramped up and

529 small-scale coal burning was banned at the end of 2017, there was still a clear spatial difference in

530 emission of air pollutants, with relatively higher $PM_{2.5}$ concentrations in the southern areas of

531 Beijing. Hence, these areas still contributed substantially to OC and EC loading in Beijing.

532 As found in earlier studies (Ji et al., 2018; Zhu et al., 2018), the southern areas of Beijing were

533 main source areas. Despite the ever-stringent air pollution control measures, which are enforced in

534 key areas of China, the economic booming in the western areas of China gave rise to substantial air

535 pollution in the adjacent areas of several provinces and the northwestern areas of China. To further

536 improve the air quality in Beijing, strict emission restrictions should be launched in the above areas

537 and joint control and prevention of air pollution should be enforced on the regional scale. It should

538 be avoided that polluted enterprises, which are closed in key regions, are moved to the western areas

539 of China or to areas where there is no supervision and control of the emission of air pollutants.

540 **4 Conclusions**

541 In this study, hourly mass concentrations of OC and EC in $PM_{2.5}$ were semi-continuously

542 measured from March 1, 2013 to February 28, 2018 at a study site in Beijing. The inter-annual,

543 monthly, seasonal and diurnal variations in OC and EC are presented, the relationship between the

544 carbonaceous species and other pollutants was examined and the source regions were assessed using

545 both NWR and PSCF analysis. The impact of the air pollution control measures and of the regional

546 transport on carbonaceous species in the fine particulate matter was investigated. The following

547 main conclusions can be drawn:

548 (1) OC and EC occupied a high fraction of the observed $PM_{2.5}$ concentrations, making it a dominant

549 contributor of $PM_{2.5}$. Their concentrations increased with the degrading air quality whereas their

550 percentage in $PM_{2.5}$ declined, which was consistent with previous studies showing that secondary

551 inorganic ions played a relatively more important role in increasing $PM_{2.5}$ concentrations.

552 (2) A clear decline in OC and EC levels was observed after a series of energy policies for air

553 pollution abatement and control had been implemented. To further improve air quality, more

554 synergistic air pollution abatement measures of carbonaceous aerosols and VOCs emissions are

555 needed.

556 (3) OC and EC showed marked seasonal, monthly, weekly and diurnal variations. The seasonal

557 patterns were characterized by higher concentrations in the colder months (from November to

558 February) and lower ones in the warm months (from May to October) of the various years. Because

559 of stringent measures for air pollution abatement, the difference between the winter and summer

560 levels decreased. The EC diurnal pattern was characterized by higher concentrations in the nighttime

561 (from 20:00 to 4:00) and lower ones in the daytime (from 9:00 to 16:00). The higher OC and EC

562 levels during the weekend can be attributed to the traffic regulation in Beijing. The diurnal

563 fluctuation in OC and EC was closely tied to a combined effect of change in emission sources and

564 evolution of the PBL.

565 (4) Significant correlations between OC and EC were observed throughout the study period,

566 suggesting that OC and EC originated from common sources, such as vehicle exhaust, coal

567 combustion, etc. The contribution of coal combustion and biomass burning decreased and this

568 resulted in lower OC/EC ratios. The OC and EC concentrations increased with higher SO_2, CO and

569 NO_x levels, while the O_3 and OC concentrations increased simultaneously for O_3 levels above 50

570 $\mu g/m^3$.

571 (5) Local emissions and regional transport played an important role in the OC and EC concentrations.

572 Higher concentrations were observed for winds from the northeast sector at wind speeds of

573 approximately 5 km/h, but there were also diffuse signals in the southwestern wind sectors,

574 highlighting probable transboundary transport from highly industrialized regions upwind of the

575 region of the Hebei province. The potential source regions of OC and EC stretched to the broader

576 areas in northwestern and western regions where coal and coal power plants are abundant. Some

577 slight differences in the potential source regions were observed from 2013 to 2017, which was

Atmospheric
Chemistry
and Physics
Discussions

578   closely associated with the economic boom in the western areas of China. In addition, the southern

579   areas of Beijing still contributed a lot to OC and EC loading in Beijing.

580   In summary, this study will be helpful for improving the understanding the sources of OC and

581   EC associated with $PM_{2.5}$ and for assessing the effectiveness of local and national PM control

582   measures. In addition, it provides valuable datasets for modelling studies and for assessing the health

583   risk.

584   **Acknowledgements**

591   **Author contributions**

592   D.S., W.M. and Y.S. designed the research. D.S., W.M., J.H., Z.W., W. K., W.P., Y.S., J.Y., B.H. and

593   Y.S. performed the research. D.S., Z.W., and W.M. analyzed the data. D.S., J.H., and W.M. wrote

594   and edited the manuscript. All other authors commented on the manuscript.

595   **References**

596   Ashbaugh, L. L., Malm, W. C., and Sadeh, W. Z.: A residence time probability analysis of sulfur

597   concentrations at Grand Canyon National Park, Atmos. Environ., 19, 1263-1270, 1985.

598   Bisht, D. S., Srivastava, A. K., Pipal, A. S., Srivastava, M. K., Pandey, A. K., Tiwari, S., and

599   Pandithurai, G.: Aerosol characteristics at a rural station in southern peninsular India during

600   CAIPEEX-IGOC: physical and chemical properties, Environ. Sci. Pollut. Res., 22, 5293-5304,

601   10.1007/s11356-014-3836-1, 2015.

602   Bond, T. C., Doherty, S. J. Fahey, D. W., Forster, P. M., Berntsen, T., DeAngelo, B. J., Flanner, M.

603   G., Ghan, S., Kärcher, B., Koch, D., Kinne, S., Kondo, Y., Quinn, P. K., Sarofim, M. C., Schultz, M.

604   G., Schulz, M., Venkataraman, C., Zhang, H., Zhang, S., Bellouin, N., Guttikunda, S. K., Hopke, P.

605   K., Jacobson, M. Z., Kaiser, J. W., Klimont, Z., Lohmann, U., Schwarz, J. P., Shindell, D., Storelvmo,

606   T., Warren, S. G., and Zender, C. S.: Bounding the role of black carbon in the climate system: A

607   scientific assessment, J. Geophys. Res-Atmos., 118(11), 5380–5552, 2013.

608   Boström, C. E., Gerde, P., Hanberg, A., Jernström, B., Johansson, C., Kyrklund, T., Rannug, A.,

609   Torngvist, M., Victorin, K., and Westerholm, R.: Cancer risk assessment, indicators, and guidelines

610   for polycyclic aromatic hydrocarbons in the ambient air, Environ. Health Perspect., 110, 451-488,

611   2002.

612   Boucher, O., Randall, D., Artaxo, P., Bretherton, C., Feingold, G., Forster, P., Kerminen, V. M.,

613   Kondo, Y., Liao, H., Lohmann, U., Rasch, P., Satheesh, S. K., Sherwood, S., Stevens, B., Zhang, X.

614   Y.: Contribution of working group | to the fifth assessment report of the Intergovernmental Panel on

615   Climate Change. Clouds and aerosols. In: Stocker, T. F., Qin, D., Plattner, G. K., Tignor, M., Allen,

616   S. K., Doschung, J., Nauels, A., Xia, Y., Bex, V., Midgley, P. M., Eds. Climate change 2013: the

617   physical science basis. Cambridge University Press, Cambridge, United Kingdom and New York,

618   616–617, 2013.

619   Bressi, M., Sciare, J., Ghersi, V., Bonnaire, N., Nicolas, J. B., Petit, J. E., Moukhtar, S., Rosso, A.,

620   and Féron, A.: A one-year comprehensive chemical characterisation of fine aerosol ($PM_{2.5}$) at urban,

621   suburban and rural background sites in the region of Paris (France), Atmos. Chem. Phys., 13(15),

622   7825-7844, 2013.

623   Cao, J. J., Lee, S. C., Zhang, X. Y., Chow, J. C., An, Z. S., Ho, K. F., Watson, J. G., Fung, K., Wang,

624   Y. Q., and Shen, Z. X.: Characterization of airborne carbonate over a site near Asian dust source

625   regions during spring 2002 and its climatic and environmental significance, J. Geophys. Res.:

626   Atmos., 110, doi:10.1029/2004JD005244, 2005.

627   Cao, J. J., Lee, S. C., Chow, J. C., Watson, J. G., Ho, K. F., Zhang, R. J., Jin, Z. D., Shen, Z. X.,

628   Chen, G. C., Kang, Y. M., Zou, S. C., Zhang, L. Z., Qi S. H., Dai, M. H., Cheng Y., and Hu, K.:

629   Spatial and seasonal distributions of carbonaceous aerosols over China, J. Geophys. Res.: Atmos.,

630   112(D22), 2007.

631   Chang, Y., Deng, C., Cao, F., Cao, C., Zou, Z., Liu, S., Lee, X., Li, J., Zhang, G., and Zhang, Y.:

632   Assessment of carbonaceous aerosols in Shanghai, China – Part 1: long-term evolution, seasonal

633   variations,   and   meteorological   effects,   Atmos.   Chem.   Phys.,   17,   9945-9964,

634   https://doi.org/10.5194/acp-17-9945-2017, 2017.

Atmospheric
Chemistry
and Physics
Discussions

635 Chen, D., Cui, H., Zhao, Y., Yin, L., Lu, Y., and Wang, Q.: A two-year study of carbonaceous

636 aerosols in ambient PM$_{2.5}$ at a regional background site for western Yangtze River Delta, China,

637 Atmos. Res., 183, 351-361, 2017.

638 Chen, Y., Xie, S., Luo, B., and Zhai, C.: Characteristics and origins of carbonaceous aerosol in the

639 Sichuan Basin, China, Atmos. Environ., 94, 215-223, 2014.

640 Chen, Y., Xie, S. D., Luo, B., and Zhai, C. Z.: Particulate pollution in urban Chongqing of southwest

641 China: Historical trends of variation, chemical characteristics and source apportionment, Sci. Total

642 Environ., 584, 523-534, 2017

643 Chen, X. C., Ward, T. J., Cao, J. J., Lee, S. C., Chow, J. C., Lau, G. N. C., Yim, S. H. L., and Ho, K.

644 F.: Determinants of personal exposure to fine particulate matter (PM$_{2.5}$) in adult subjects in Hong

645 Kong, Sci. Total Environ., 628-629, 1165-1177, https://doi.org/10.1016/j.scitotenv.2018.02.049,

646 2018.

647 Cheng, N., Chen, Z., Sun, F., Sun, R., Dong, X., Xie, X., and Xu, C.: Ground ozone concentrations

648 over Beijing from 2004 to 2015: Variation patterns, indicative precursors and effects of emission

649 reduction, Environ. Pollut., 237, 262-274, https://doi.org/10.1016/j.envpol.2018.02.051, 2018.

650 Chow, J. C., Watson, J. G., Lu, Z., Lowenthal, D. H., Frazier, C. A., Solomon, P. A., Thuillier, R. H.,

651 and Magliano, K.: Descriptive analysis of PM$_{2.5}$ and PM$_{10}$ at regionally representative locations

652 during SJVAQS/AUSPEX, Atmos. Environ., 30, 2079-2112, https://doi.org/10.1016/1352-

653 2310(95)00402-5, 1996.

654 Dai, Q. L., Bi, X. H., Liu, B. S., Li, L. W., Ding, J., Song, W. B., Bi, S. Y., Schulze, B. C., Song, C.

655 B., Wu, J. H., Zhang, Y. F., Feng, Y. C., and Hopke, P. K.: Chemical nature of PM$_{2.5}$ and PM$_{10}$ in

656 Xi'an, China: Insights into primary emissions and secondary particle formation, Environ. Pollut.

657 240, 155-166, 2018.

658 Dan, M., Zhuang, G., Li, X., Tao, H., and Zhuang, Y.: The characteristics of carbonaceous species

659 and their sources in PM$_{2.5}$ in Beijing, Atmos. Environ., 38, 3443-3452,

660 https://doi.org/10.1016/j.atmosenv.2004.02.052, 2004.

661 Ding, A. J., Huang, X., Nie, W., Sun, J. N., Kerminen, V. M., Petäjä, T., Su, H., Cheng, Y. F., Yang,

662 X. Q., Wang, M. H., Chi, X. G., Wang, J. P., Virkkula, A., Guo, W. D., Yuan, J., Wang, S. Y.,

663 Zhang, R. J., Wu, Y. F., Song, Y., Zhu, T., Zilitinkevich, S., Kulmala, M., and Fu, C. B.: Enhanced

664   haze pollution by black carbon in megacities in China, Geophys. Res. Lett., 43, 2873–2879, 2016.

665   Duan, F., He, K., Ma, Y., Yang, F., Yu, X., Cadle, S., Chan, T., and Mulawa, P.: Concentration and

666   chemical characteristics of $PM_{2.5}$ in Beijing, China: 2001–2002, Sci. Total Environ., 355, 264-275,

667   2006.

668   Gao, J., Woodward, A., Vardoulakis, S., Kovats, S., Wilkinson, P., Li, L., Xu, L., Li, J., Yang, J., Li,

669   J., Cao, L., Liu, X., Wu, H., and Liu, Q.: Haze, public health and mitigation measures in China: A

670   review of the current evidence for further policy response, Sci. Total Environ., 578, 148-157,

671   https://doi.org/10.1016/j.scitotenv.2016.10.231, 2017.

672   Grivas, G., Cheristanidis, S., and Chaloulakou, A.: Elemental and organic carbon in the urban

673   environment of Athens. Seasonal and diurnal variations and estimates of secondary organic carbon,

674   Sci. Total Environ., 414, 535-545, 2012.

675   Hassler, B., McDonald, B. C., Frost, G. J., Borbon, A., Carslaw, D. C., Civerolo, K., Granier, C.,

676   Monks, P. S., Monks, S., Parrish, D. D., Pollack, I. B., Rosenlof, K. H., Ryerson, T. B.,

677   Schneidemesser, E., and Trainer, M.: Analysis of long-term observations of NOx and CO in

678   megacities and application to constraining emissions inventories, Geophys. Res. Lett., 43, 9920-

679   9930, doi:10.1002/2016GL069894, 2016.

680   He, K., Yang, F., Ma, Y., Zhang, Q., Yao, X., Chan, C. K., Cadle, S., Chan, T., and Mulawa, P.: The

681   characteristics of $PM_{2.5}$ in Beijing, China, Atmos. Environ., 35, 4959-4970,

682   https://doi.org/10.1016/S1352-2310(01)00301-6, 2001.

683   Henry, R., Norris, G. A., Vedantham, R., and Turner, J. R.: Source region identification using

684   Kernel smoothing, Environ. Sci. Technol., 43 (11), 4090-4097, http://dx.doi.org/10.1021/

685   es8011723, 2009.

686   Hu, G., Sun, J., Zhang, Y., Shen, X., and Yang, Y.: Chemical composition of $PM_{2.5}$ based on two-

687   year measurements at an urban site in Beijing. Aerosol Air Qual. Res, 15, 1748-1759, 2015.

688   Ji, D., Wang, Y., Wang, L., Chen, L., Hu, B., Tang, G., Xin, J. Y., Song, T., Wen, T. X., Sun, Y., Pan,

689   Y. P., and Liu, Z. R., Analysis of heavy pollution episodes in selected cities of northern China, Atmos.

690   Environ., 50, 338-348, 2012.

691   Ji, D., Li, L., Wang, Y., Zhang, J., Cheng, M., Sun, Y., Liu, Z. R., Wang, L. L., Tang, G. Q., Hu, B.,

692   Chao, N., Wen, T. X., and Miao, H. Y.: The heaviest particulate air-pollution episodes occurred in

Atmospheric
Chemistry
and Physics
Discussions

693   northern China in January, 2013: Insights gained from observation, Atmos. Environ., 92, 546-556,

694   2014.

695   Ji, D. S., Zhang, J. K., He, J., Wang, X. J., Pang, B., Liu, Z. R., Wang, L. L., and Wang, Y. S.:

696   Characteristics of atmospheric organic and elemental carbon aerosols in urban Beijing, China,

697   Atmos. Environ., 125, 293-306, 2016.

698   Ji, D. S., Yan, Y. C., Wang, Z. S., He, J., Liu, B., Sun, Y., Gao, M., Li, Y., Cao, W., Cui, Y., Hu, B.,

699   Xin, J. Y., Wang, L. L., Liu, Z. R., Tang, G. Q., and Wang, Y. S.: Two-year continuous measurements

700   of carbonaceous aerosols in urban Beijing, China: Temporal variations, characteristics and source

701   analyses, Chemosphere, 200, 191-200, 2018.

702   Jin, Y., Andersson, H., and Zhang, S.: Air pollution control policies in China: a petrospective and

703   prospects, Int. J. Env. Res. Pub. He., 13(12), 1219, 2016.

704   Jeong, B., Bae, M. S., Ahn, J., and Lee, J.: A study of carbonaceous aerosols measurement in

705   metropolitan area performed during Korus-AQ 2016 campaign, J. Kor. Soc. Atmos. Environ., 33,

706   2017.

707   Lang, J., Zhang, Y., Zhou, Y., Cheng, S., Chen, D., Guo, X., Chen, S., Li, X. X., Xing, X. F., and

708   Wang, H. Y.: Trends of $PM_{2.5}$ and chemical composition in Beijing, 2000-2015. Aerosol Air Qual.

709   Res., 17, 412-425, 2017.

710   Li, B., Zhang, J., Zhao, Y., Yuan, S., Zhao, Q., Shen, G., and Wu, H.: Seasonal variation of urban

711   carbonaceous aerosols in a typical city Nanjing in Yangtze River Delta, China, Atmos. Environ.,

712   106, 223-231, 2015.

713   Li, C., Chen, P., Kang, S., Yan, F., Hu, Z., Qu, B., and Sillanpää, M.: Concentrations and light

714   absorption characteristics of carbonaceous aerosol in $PM_{2.5}$ and PM_{10} of Lhasa city, the Tibetan

715   Plateau, Atmos. Environ., 127, 340-346, https://doi.org/10.1016/j.atmosenv.2015.12.059, 2016.

716   Li, C., McLinden, C., Fioletov, V., Krotkov, N., Carn, S., Joiner, J., Streets, D., He, H., Ren, X., Li,

717   Z., and Dickerson, R.: India is overtaking China as the world's largest emitter of anthropogenic

718   sulfur dioxide, Scientific Reports, DOI:10.1038/s41598-017-14639-8, 2017.

719   Li, Y. C., Shu, M., Ho, S. S. H., Yu, J. Z., Yuan, Z. B., Liu, Z. F., Wang, X. X., and Zhao, X, Q.:

720   Effects of Chemical Composition of $PM_{2.5}$ on Visibility in a Semi-rural City of Sichuan Basin,

721   Aerosol and Air Qual. Res., 18(4): 957-968, 2018.

Atmospheric
Chemistry
and Physics
Discussions

722   Liang, Q., Jaeglé, L., Jaffe, D. A., Weiss-Penzias, P., Heckman, A., and Snow, J. A.: Long-range

723   transport of Asian pollution to the northeast Pacific: Seasonal variations and transport pathways of

724   carbon monoxide, J. Geophys. Res-Atmos., 109, doi:10.1029/2003JD004402, 2004.

725   Liu, D., Li, J., Zhang, Y., Xu, Y., Liu, X., Ding, P., Shen, C., Chen, Y., Tian, C., and Zhang, G.: The

726   use of levoglucosan and radiocarbon for source apportionment of $PM_{2.5}$ carbonaceous aerosols at a

727   background site in east China, Environ. Sci. Technol., 47, 10454, 2013.

728   Liu, F., Zhang, Q., Tong, D., Zheng, B., Li, M., Huo, H., and He, K. B.: High-resolution inventory

729   of technologies, activities, and emissions of coal-fired power plants in China from 1990 to 2010,

730   Atmos. Chem. Phys., 15, 13299-13317, https://doi.org/10.5194/acp-15-13299-2015, 2015.

731   Liu, G., Li, J., Wu, D., and Xu, H.: Chemical composition and source apportionment of the ambient

732    $PM_{2.5}$ in Hangzhou, China, Particuology, 18, 135-143, 2015.

733   Lupu A. and Maenhaut, W.: Application and comparison of two statistical trajectory techniques for

734   identification of source regions of atmospheric aerosol species, Atmos. Environ., 36, 5607-5618,

735   2002.

736   Lv, B., Zhang, B., and Bai, Y.: A systematic analysis of $PM_{2.5}$ in Beijing and its sources from 2000

737   to 2012. Atmos. Environ., 124, 98-108, 2016.

738   Malm, W. C., Sisler, J. F., Huffman, D., Eldred, R. A., and Cahill, T. A.: Spatial and seasonal trends

739   in particle concentration and optical extinction in the United States, J. Geophys. Res-Atmos., 99,

740   1347-1370, doi:10.1029/93JD02916, 1994.

741   Miyakawa, T., Kanaya, Y., Komazaki, Y., Miyoshi, T., Nara, H., Takami, A., Moteki, N., Koike, M.,

742   and Kondo, Y.: Emission regulations qltered the concentrations, origin, and formation of

743   carbonaceous aerosols in the Tokyo metropolitan area, Aerosol Air Qual. Res., 16, 1603-1614,

744   10.4209/aaqr.2015.11.0624, 2016.

745   Na, K., Sawant, A. A., Song, C., and Cocker, D. R.: Primary and secondary carbonaceous species

746   in the atmosphere of Western Riverside County, California, Atmos. Environ., 38, 1345-1355,

747   https://doi.org/10.1016/j.atmosenv.2003.11.023, 2004.

748   Niu, X. Y., Cao, J. J., Shen, Z. X., Ho, S. S. H., Tie, X. X., Zhao, S. Y., Xue, H. M., Zhang, T., and

749   Huang, R. J.: $PM_{2.5}$ from the Guanzhong Plain: Chemical composition and implications for emission

750   reductions, Atmos. Environ., 147, 458-469, 2016.

751   Paraskevopoulou, D., Liakakou, E., Gerasopoulos, E., Theodosi, C., and Mihalopoulos, N.: Long-

752   term characterization of organic and elemental carbon in the PM$_{2.5}$ fraction: the case of Athens,

753   Greece, Atmos. Chem. Phys., 14(23), 13313-13325, 2014.

754   Park, J. S., Song, I. H., Park, S. M., Shin, H., and Hong, Y.: The characteristics and seasonal

755   variations of OC and EC for PM$_{2.5}$ in Seoul metropolitan area in 2014, J. Environ. Impact Assess.,

756   24, 578-592, 2015.

757   Peltier, R. E., Weber, R. J., and Sullivan, A. P.: Investigating a liquid-based method for online

758   organic carbon detection in atmospheric particles, Aerosol Sci. Tech., 41, 1117-1127,

759   10.1080/02786820701777465, 2007.

760   Pereira, G. M., Teinilä, K., Custódio, D., Santos, A. G., Xian, H., Hillamo, R., Alves, C. A., Andrade,

761   J. B., Rocha, G. O., Kumar, P., Balasubramanian, R., Andrade M. F., and Vasconcellos, P. C.:

762   Airborne particles in the Brazilian city of São Paulo: One-year investigation for the chemical

763   composition and source apportionment, Atmos. Chem. Phys., 17, 11943-11969, 2017.

764   Petit, J. E., Favez, O., Albinet, A., and Canonaco, F.: A user-friendly tool for comprehensive

765   evaluation of the geographical origins of atmospheric pollution: Wind and trajectory analyses.

766   Environ. Modell. Softw., 88, 183-187, 2017.

767   Poirot, R. L. and Wishinski, P. R.: Visibility, sulfate and air mass history associated with the

768   summertime aerosol in northern Vermont, Atmos. Environ., 20, 1457-1469, 1986.

769   Polissar, A. V., Hopke, P. K., and Harris, J. M.: Source regions for atmospheric aerosol measured at

770   Barrow, Alaska, Environ. Sci. Technol., 35, 4214-4226, 2001.

771   Ram, K. and Sarin, M. M.: Spatio-temporal variability in atmospheric abundances of EC, OC and

772   WSOC   over   Northern   India,   J.   Aerosol   Sci.,   41,   88-98,

773   https://doi.org/10.1016/j.jaerosci.2009.11.004, 2010.

774   Ram, K. and Sarin, M.: Carbonaceous aerosols over Northern India: sources and spatio-temporal

775   variability, Proc. Indian Natn. Sci. Acad., 78, 523-533, 2012.

776   Ren, Z. H., Wan, B. T., Yu, T., Su, F. Q., Zhang, Z. G., Gao, Yang, X. X., Hu, H. L., Wu, Y. H., Hu,

777   F., and Hong, Z. X.: Influence of weather system of different scales on pollution boundary layer and

778   the transport in horizontal current field, Res. Environ. Sci, 17(1), 7-13, 2004.

779   Schauer, J. J., Kleeman, M. J., Cass, G. R., and Simoneit, B. R.: Measurement of emissions from

780   air pollution sources. 5. C1-C32 organic compounds from gasoline-powered motor vehicles,

781   Environ. Sci. Technol., 36, 1169–1180, 2002.

782   Seinfeld, J. H. and Pandis, S. N.: Atmospheric chemistry and physics: from air pollution to climate

783   change, John Wiley & Sons, 1998.

784   Shah, J. J., Johnson, R. L., Heyerdahl, E. K., and Huntzicker, J. J.: Carbonaceous aerosol at urban

785   and rural sites in the United States, J. Air Pollut. Control Assoc., 36, 254-257, 1986.

786   Sharma, S. K. and Mandal, T. K.: Chemical composition of fine mode particulate matter ($PM_{2.5}$) in

787   an urban area of Delhi, India and its source apportionment, Urban Clim., 21, 106-122,

788   https://doi.org/10.1016/j.uclim.2017.05.009, 2017.

789   Shi, G. L., Peng, X., Liu, J. Y., Tian, Y. Z., Song, D. L., Yu, H. F., Feng, Y. C., and Russell, A. G.:

790   Quantification of long-term primary and secondary source contributions to carbonaceous aerosols,

791   Environ. Pollut. 219, 897-905, 2016.

792   Sofowote, U. M., Rastogi, A. K., Debosz, J., and Hopke, P. K.: Advanced receptor modeling of

793   near–real–time, ambient $PM_{2.5}$ and its associated components collected at an urban–industrial site

794   in Toronto, Ontario, Atmos. Pollut. Res., 5, 13-23, https://doi.org/10.5094/APR.2014.003, 2014.

795   Song, Y., Xie, S., Zhang, Y., Zeng, L., Salmon, L. G., and Zheng, M.: Source apportionment of

796    $PM_{2.5}$ in Beijing using principal component analysis/absolute principal component scores and

797   UNMIX, Sci. Total Environ., 372, 278-286, 2006.

798   Tao, J., Cheng, T., Zhang, R., Cao, J., Zhu, L., Wang, Q., Luo, L., and Zhang, L.: Chemical

799   composition of $PM_{2.5}$ at an urban site of Chengdu in southwestern China, Adv. Atmos. Sci., 30,

800   1070-1084, 2013.

801   Tao, J., Gao, J., Zhang, L., Zhang, R., Che, H., Zhang, Z., Lin, Z., Jing, J., Cao, J., and Hsu, S. C.:

802    $PM_{2.5}$ pollution in a megacity of southwest China: source apportionment and implication, Atmos.

803   Chem. Phys., 14, 2014.

804   Tao, J., Zhang, L., Cao, J., and Zhang, R.: A review of current knowledge concerning $PM_{2.5}$

805   chemical composition, aerosol optical properties and their relationships across China, Atmos. Chem.

806   Phys., 17(15), 9485-9518, 2017.

807   Villalobos, A. M., Amonov, M. O., Shafer, M. M., Devi, J. J., Gupta, T., Tripathi, S. N., Rana, K. S.,

808   McKenzie, M., Bergin, M. H., and Schauer, J. J.: Source apportionment of carbonaceous fine

809   particulate matter (PM$_{2.5}$) in two contrasting cities across the Indo–Gangetic Plain, Atmos. Pollut.

810   Res., 6, 398-405, https://doi.org/10.5094/APR.2015.044, 2015.

811   Wang, J., Allen, D. J., Pickering, K. E., Li, Z., and He, H.: Impact of aerosol direct effect on East

812   Asian air quality during the EAST-AIRE campaign, J. Geophys. Res-Atmos., 121(11), 6534-6554,

813   2016b.

814   Wang, L., Zhou, X., Ma, Y., Cao, Z., Wu, R., and Wang, W.: Carbonaceous aerosols over China-

815   review of observations, emissions, and climate forcing, Environ. Sci. Pollut. Res., 23(2), 1671-1680,

816   2016a.

817   Wang, P., Cao, J. J., Shen, Z. X., Han, Y. M., Lee, S. C., Huang, Y., Zhu, C. S., Wang, Q. Y., Xu, H.

818   M., and Huang, R. J.: Spatial and seasonal variations of PM$_{2.5}$ mass and species during 2010 in Xi'an,

819   China, Sci. Total Environ., 508, 477-487, https://doi.org/10.1016/j.scitotenv.2014.11.007, 2015.

820   Wang, Y., Khalizov, A., Levy, M., and Zhang, R. Y.: New Directions: light absorbing aerosols and

821   their atmospheric impacts, Atmos. Environ., 81, 713–715, 2013.

822   Wang, Y. Q., Zhang, X. Y., and Draxler, R. R.: TrajStat: GIS-based software that uses various

823   trajectory statistical analysis methods to identify potential sources from long-term air pollution

824   measurement data, Environ. Modell. Softw., 24(8), 938-939, 2009.

825   Wang, Z. S., Zhang, D. W., Liu, B. X., Li, Y. T., Chen, T., Sun, F., Yang, D. Y., Liang, Y. P., Chang,

826   M., Liu, Y., and Lin, A. G.: Analysis of chemical characteristics of PM$_{2.5}$ in Beijing over a 1-year

827   period, J. Atmos. Chem., 73(4): 407-425, 2016c.

828   WHO. Health effects of black carbon. http://wedocs.unep.org/handle/20.500.11822/8699, 2012.

829   Wu, C., Wu, D., and Yu, J. Z.: Quantifying black carbon light absorption enhancement with a novel

830   statistical approach, Atmos. Chem. Phys., 18, 289-309, https://doi.org/10.5194/acp-18-289-2018,

831   2018.

832   Wu, D., Liao B. T, Wu M., Chen, H., Wang, Y., Niao, X., Gu, Y., Zhang, X., Zhao, X. J., Quan, J.

833   N., Liu, W. D., Meng, J., and Sun, D.: The long-term trend of haze and fog days and the surface

834   layer transport conditions under haze weather in North China, Acta Sci Circumst., 34, 1-11, 2014.

835   Wu, H., Zhang, Y. F., Han, S. Q., Wu, J. H., Bi, X. H., Shi, G. L., Wang, J., Yao, Q., Cai, Z. Y., Liu,

836   J. L., and Feng, Y. C.: Vertical characteristics of PM$_{2.5}$ during the heating season in Tianjin, China,

837   Sci. Total Environ., 523, 152-160, https://doi.org/10.1016/j.scitotenv.2015.03.119, 2015.

Wu, X., Wu, Y., Zhang, S., Liu, H., Fu, L., and Hao, J.: Assessment of vehicle emission programs in China during 1998–2013: achievement, challenges and implications, Environ. Pollut., 214, 556-567, 2016.

Xing, J., Wang, J., Mathur, R., Wang, S., Sarwar, G., Pleim, J., Hogrefe, C., Zhang, Y., Jiang, J., Wong, D. C., and Hao, J.: Impacts of aerosol direct effects on tropospheric ozone through changes in atmospheric dynamics and photolysis rates, Atmos. Chem. Phys., 17, 9869-9883, 2017.

Xu, J., Wang, Q., Deng, C., McNeill, V. F., Fankhauser, A., Wang, F., Zheng, X., Shen, J., Huang, K., and Zhuang, G.: Insights into the characteristics and sources of primary and secondary organic carbon: High time resolution observation in urban Shanghai, Environ. Pollut., 233, 1177-1187, https://doi.org/10.1016/j.envpol.2017.10.003, 2018.

Yang, F., He, K., Ye, B., Chen, X., Cha, L., Cadle, S.H., Chan, T., and Mulawa, P. A.: One-year record of organic and elemental carbon in fine particles in downtown Beijing and Shanghai, Atmos. Chem. Phys., 5, 1449–1457, 2005.

Yang, F., Huang, L., Duan, F., Zhang, W., He, K., Ma, Y., Brook, J. R., Tan, J., Zhao, Q., and Cheng, Y.: Carbonaceous species in $PM_{2.5}$ at a pair of rural/urban sites in Beijing, 2005-2008, Atmos. Chem. Phys., 11, 7893–7903, 2011a.

Yang, F., Tan, J., Zhao, Q., Du, Z., He, K., Ma, Y., Duan, F., and Chen, G.: Characteristics of $PM_{2.5}$ speciation in representative megacities and across China, Atmos. Chem. Phys., 11, 5207-5219, 2011b.

Yu, X. Y., Cary, R. A., and Laulainen, N. S.: Primary and secondary organic carbon downwind of Mexico City, Atmos. Chem. Phys., 9(18), 6793-6814, 2009.

Zhang, F., Zhao, J., Chen, J., Xu, Y., and Xu, L.: Pollution characteristics of organic and elemental carbon in $PM_{2.5}$ in Xiamen, China, J. Environ. Sci., 23(8), 1342-1349, 2011.

Zhang, R., Jing, J., Tao, J., Hsu, S. C., Wang, G., Cao, J., Lee, C. S. L., Zhu, L., Chen, Z., Zhao, Y., and Shen Z.: Chemical characterization and source apportionment of $PM_{2.5}$ in Beijing: seasonal perspective, Atmos. Chem. Phys., 13, 7053–7074, 2013.

Zhang, R. Y., Khalizov, A. F., Pagels, J., Zhang, D., Xue, H., and McMurry, P. H.: Variability in morphology, hygroscopicity, and optical properties of soot aerosols during atmospheric processing, Proc. Natl. Acad. Sci. U.S.A., 105, 10291–10296, 2008.

Atmospheric
Chemistry
and Physics
Discussions

867   Zhang, F., Wang, Z. W., Cheng, H. R., Lv, X. P., Gong, W., Wang, X. M., and Zhang, G.: Seasonal

868   variations and chemical characteristics of PM$_{2.5}$ in Wuhan, central China, Sci. Total Environ., 518-

869   519, 97-105, https://doi.org/10.1016/j.scitotenv.2015.02.054, 2015.

870   Zhang, Y., Li, C., Krotkov, N. A., Joiner, J., Fioletov, V., and McLinden, C.: Continuation of long-

871   term global SO$_2$ pollution monitoring from OMI to OMPS, Atmos. Meas. Tech., 10, 1495-1509,

872   https://doi.org/10.5194/amt-10-1495-2017, 2017.

873   Zhang, Y., Zhang, Q., Cheng, Y., Su, H., Li, H., Li, M., Zhang, X., Ding, A., and He, K.:

874   Amplification of light absorption of black carbon associated with air pollution, Atmos. Chem. Phys.,

875   18, 9879-9896, https://doi.org/10.5194/acp-18-9879-2018, 2018.

876   Zhao, P., Dong, F., and Yang, Y.: Characteristics of carbonaceous aerosol in the region of Beijing,

877   Tianjin, and Hebei, China, Atmos. Environ., 71, 389-398, 2013.

878   Zhao, M., Huang, Z., Qiao, T., Zhang, Y., Xiu, G., and Yu, J.: Chemical characterization, the

879   transport pathways and potential sources of PM$_{2.5}$ in Shanghai: Seasonal variations, Atmos. Res.,

880   158, 66-78, 2015a.

881   Zhao, M., Qiao, T., Huang, Z., Zhu, M., Xu, W., Xiu, G., Tao, J., and Lee, S.: Comparison of ionic

882   and carbonaceous compositions of PM$_{2.5}$ in 2009 and 2012 in Shanghai, China, Sci. Total Environ.,

883   536, 695-703, 2015b.

884   Zheng, B., Tong, D., Li, M., Liu, F., Hong, C., Geng, G., Li, H. Y., Li, X., Peng, L. Q., Qi, J., Yan,

885   L., Zhang, Y. X., Zhao, H. Y., Zheng, Y. X., He, K. B., and Zhang, Q.: Trends in China's

886   anthropogenic emissions since 2010 as the consequence of clean air actions, Atmos. Chem. Phys.,

887   18, 14095–14111, 2018.

888   Zheng, G. J., Duan, F. K., Su, H., Ma, Y. L., Cheng, Y., Zheng, B., Zheng, B., Zhang, Q., Huang, T.,

889   Kimoto, T., Chang, D., Pöschl, U., Cheng, Y. F., and He, K. B.: Exploring the severe winter haze in

890   Beijing: the impact of synoptic weather, regional transport and heterogeneous reactions, Atmos.

891   Chem. Phys. 15(6), 2969-2983, 2015.

892   Zhu, C., Tian, H., Hao, Y., Gao, J., Hao, J., Wang, Y., Hua, S., Wang, K., and Liu, H.: A high-

893   resolution emission inventory of anthropogenic trace elements in Beijing-Tianjin-Hebei (BTH)

894   region of China, Atmos. Environ., 191, 452-462, https://doi.org/10.1016/j.atmosenv.2018.08.035,

895   2018.
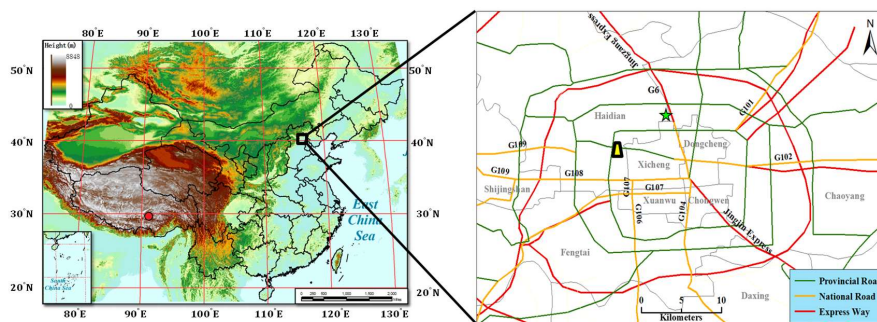
896

897   Fig. 1. Map with location of the sampling site (the trapezoidal symbol in the right figure indicates

898   the sampling site).
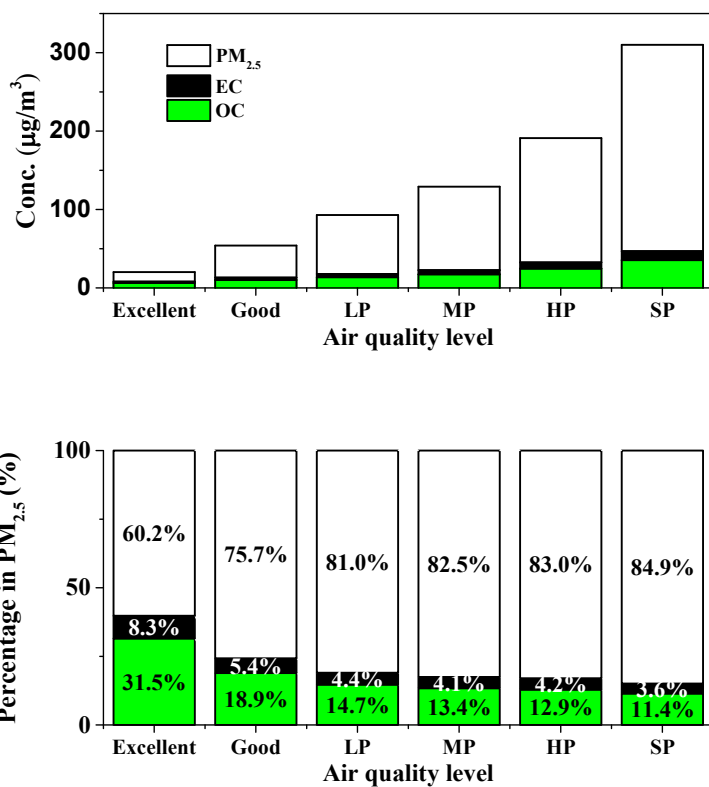
899
900
901

902   Fig. 2. Variation of OC, EC, and PM$_{2.5}$ concentrations and of the percentages of OC, EC, and other
903   components in PM$_{2.5}$ for different air quality levels.

904

905
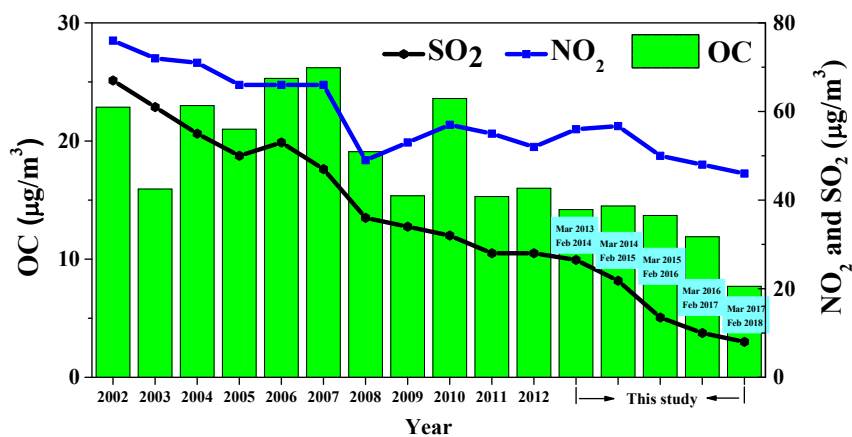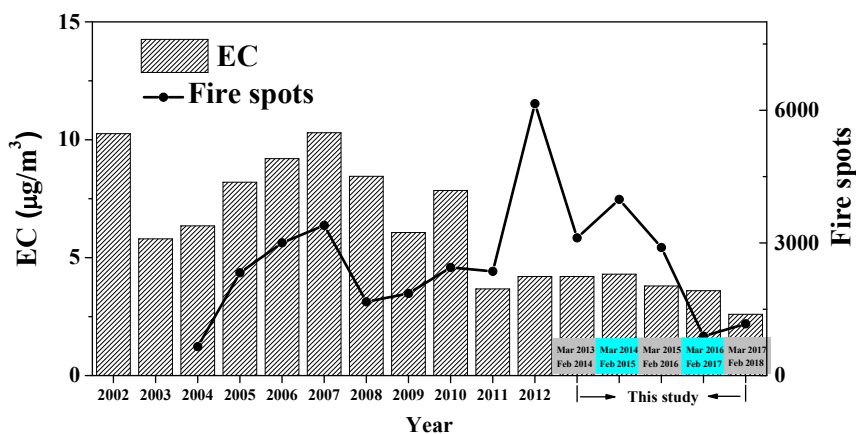
Fig. 3. Inter-annual variation in the annual mean OC and EC concentrations in $PM_{2.5}$ from 2002 to
2018 in Beijing. The variation in NO_2 and SO_2 concentrations and in the number of fire spots is also
shown.

909

910
911

912

913
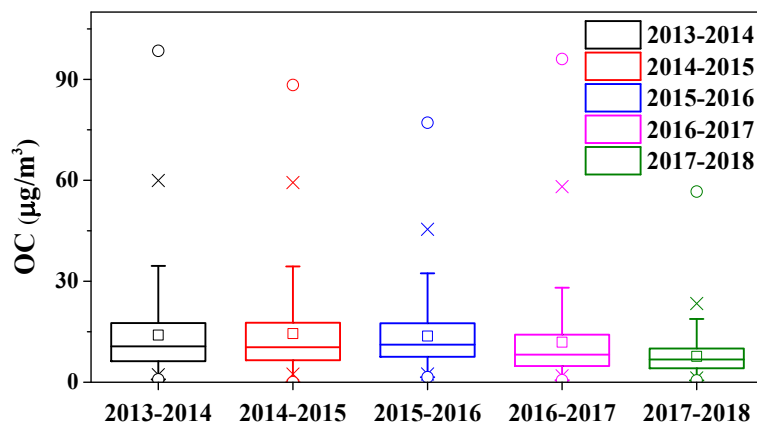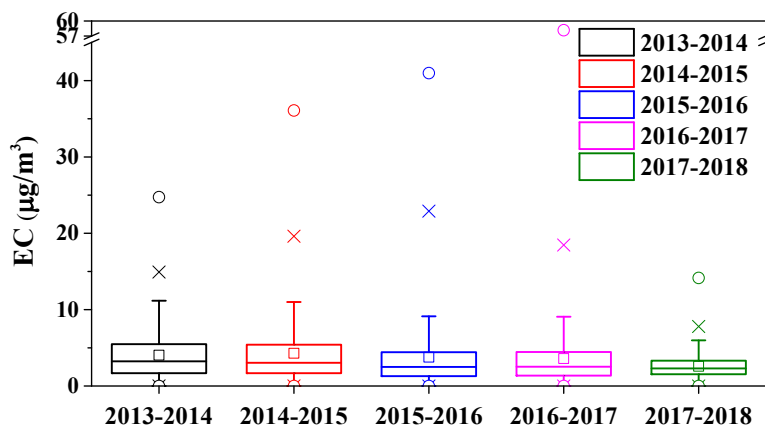
Fig. 4. Interannual variation of OC and EC during the whole study period.

915

916
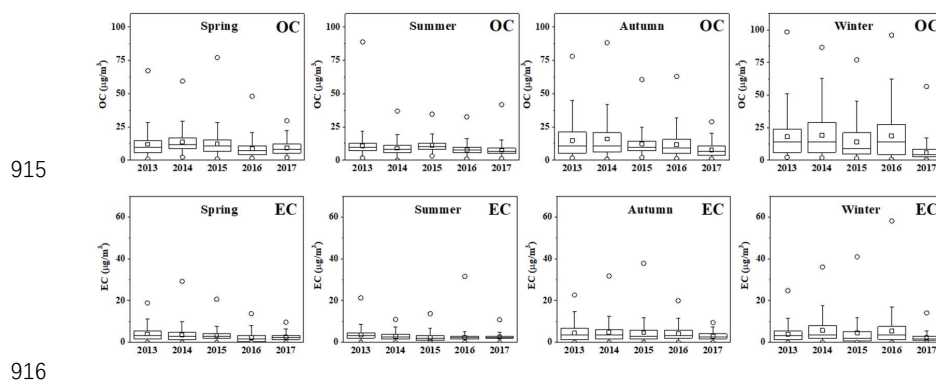
917   Fig. 5. Seasonal variations of OC and EC concentrations from March 2013 to February 2018.

918
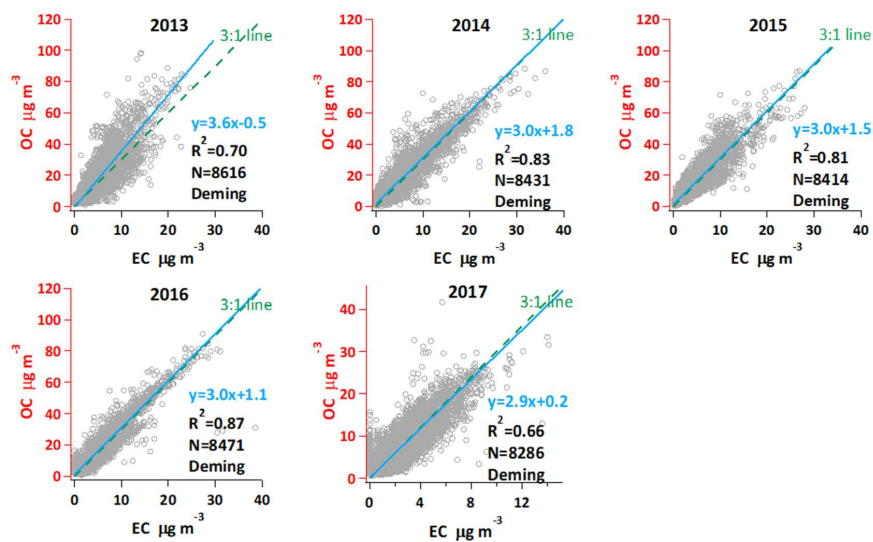
Fig. 6. Relationship between OC and EC using the Deming regression method from 2013 to 2017
(the dashed line indicates a OC/EC ratio of 3:1).
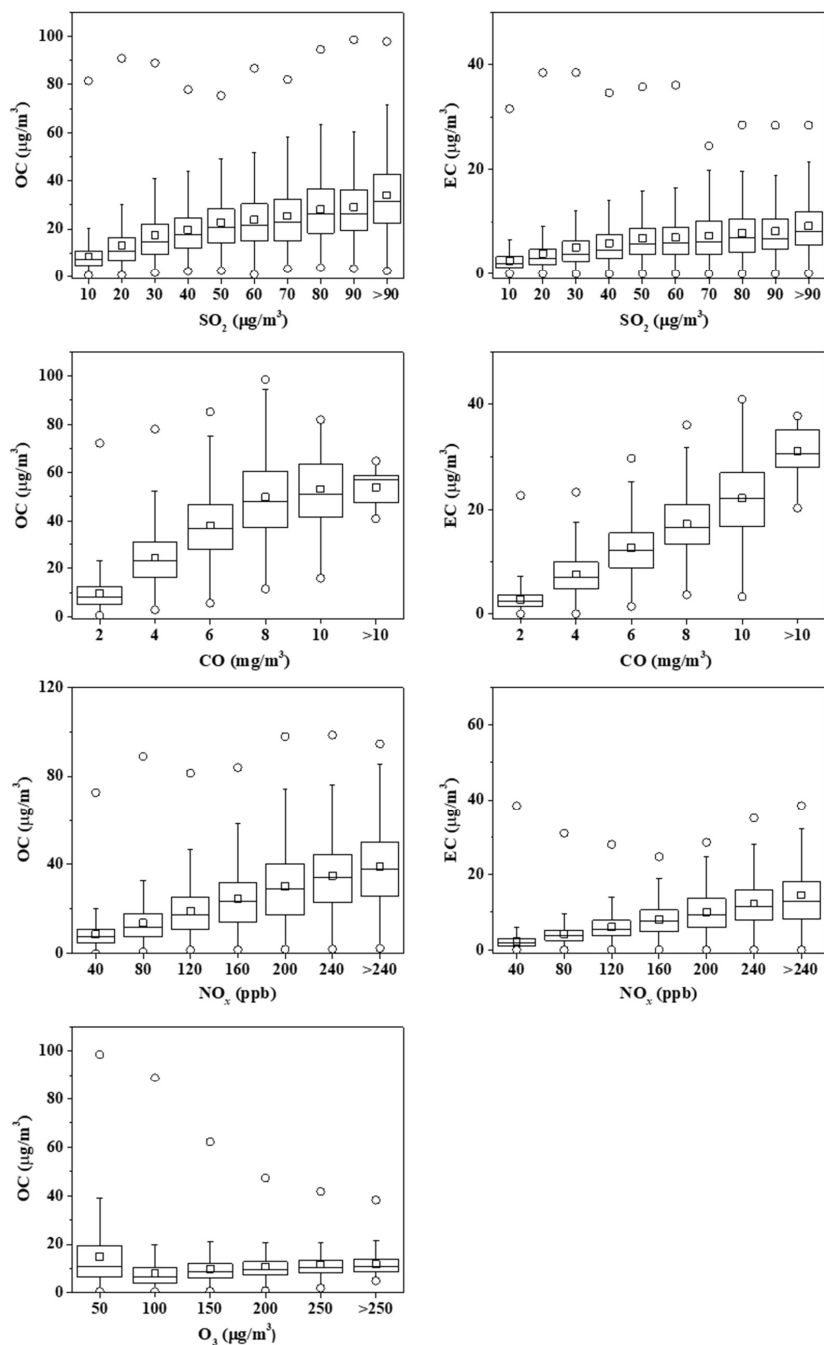
921

922   Fig. 7. OC and EC concentrations as a function of the SO_2, CO, NO_x and O_3 concentration.

923
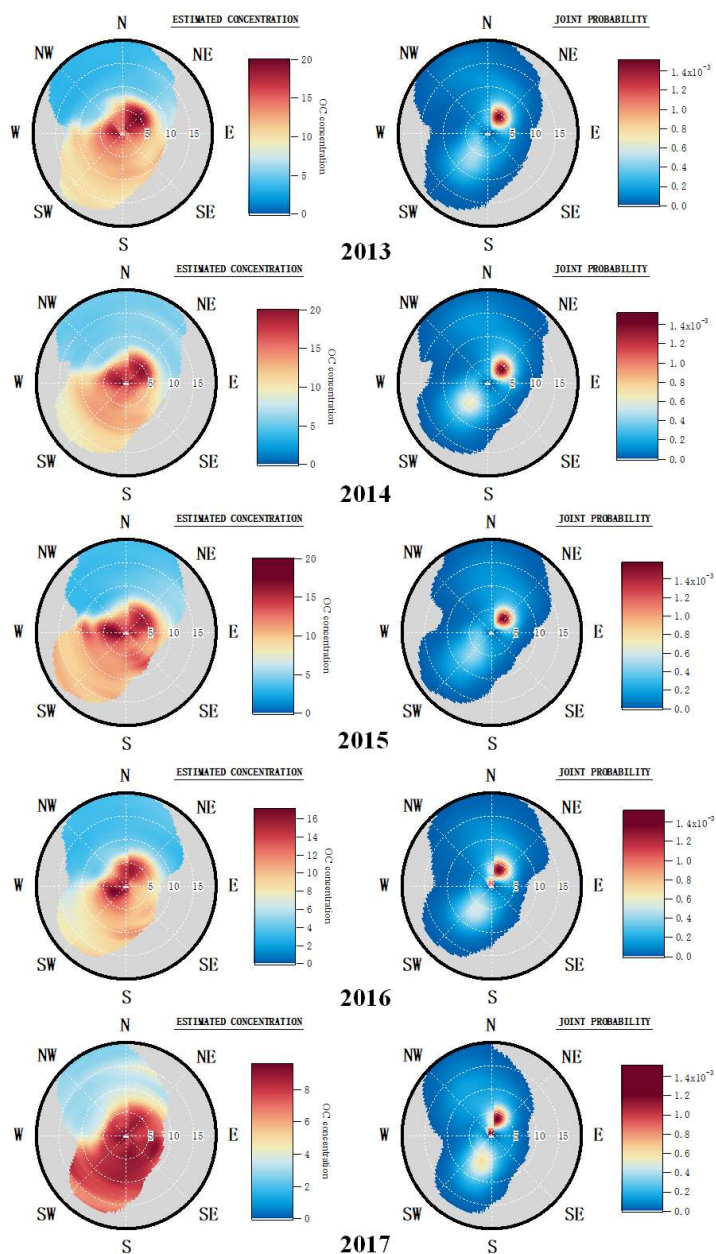
Fig. 8. Wind analysis results using NWR on 1-h OC concentrations measured in Beijing from 2013
to 2017 (Unit of wind speed: km/h).

Atmospheric
Chemistry
and Physics
Discussions
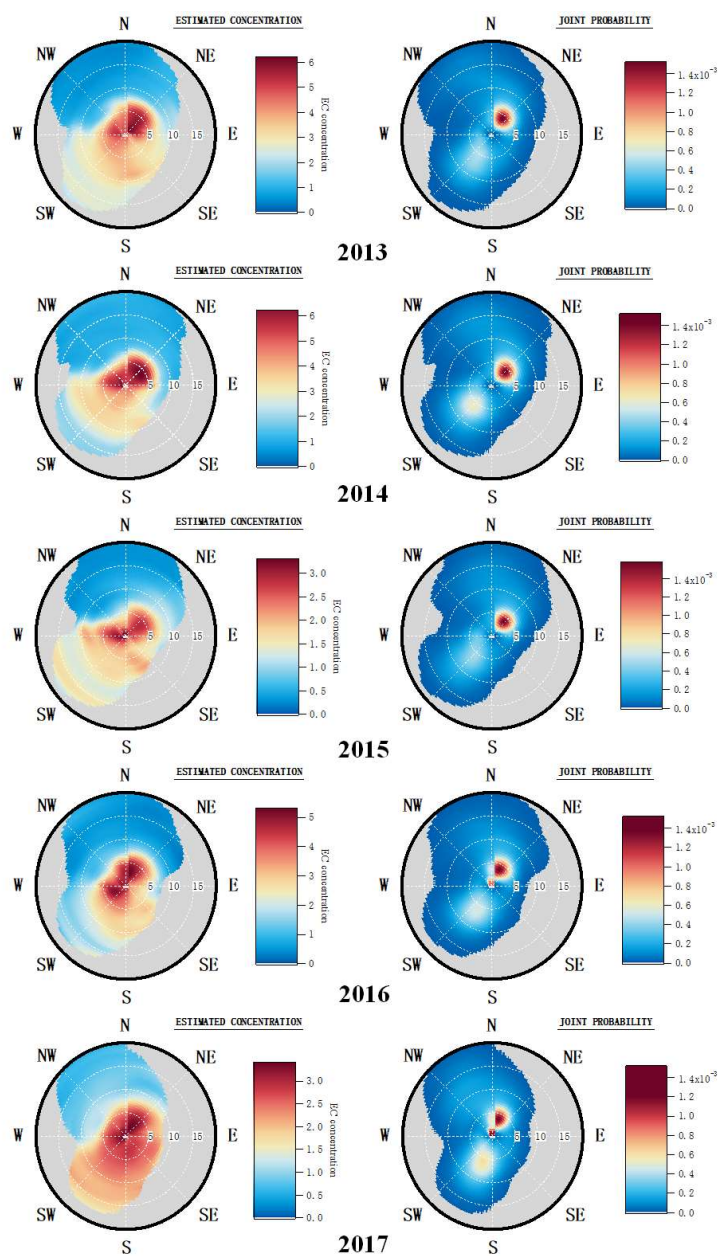
926

927   Fig. 9. Wind analysis results using NWR on 1-h EC concentrations measured in Beijing from 2013
928   to 2017.

929
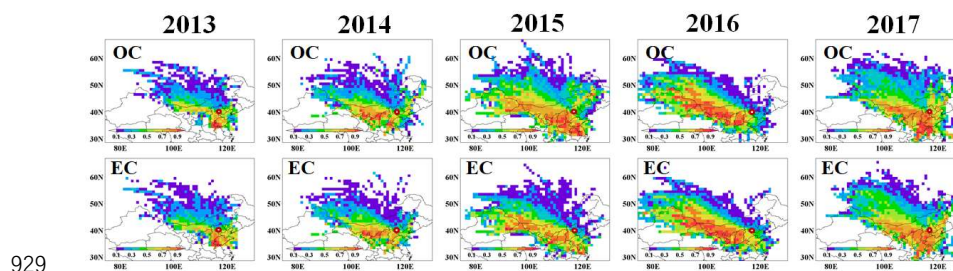
930 Fig. 10 Potential source areas for OC and EC in Beijing from 2013 to 2017. The color code denotes

931 the PSCF probability. The measurement site is indicated with a ◯. The identification of the

932 provinces is given in Fig. S9.

Atmospheric
Chemistry
and Physics
Discussions

933   Table 1. Statistics for the OC and EC concentrations (in $\mu g/m^3$) from March 2013 to February 2018.

	OC	Stdev	EC	Stdev	PM$_{2.5}$	Stdev	OC/PM$_{2.5}$	EC/PM$_{2.5}$	TC/PM$_{2.5}$
Mar-2013－Feb-2014	14.0	11.7	4.0	3.3	89.0	82.9	0.157	0.045	0.203
Mar-2014－Feb-2015	14.5	12.1	4.3	4.0	85.5	76.6	0.169	0.050	0.219
Mar-2015－Feb-2016	13.7	9.2	3.8	4.4	76.9	85.6	0.178	0.049	0.228
Mar-2016－Feb-2017	11.9	11.3	3.6	3.7	79.4	82.8	0.150	0.045	0.195
Mar-2017－Feb-2018	7.7	4.7	2.6	1.6	49.4	48.6	0.155	0.052	0.208
whole study period	12.4	10.6	3.7	3.6	75.7	77.6	0.164	0.049	0.213

934

935 Table 2. Annual variations of gross domestic product, population, total energy consumption, population of vehicles, consumption of gasoline, diesel oil, coal,

936 natural gas and vehicle emission standards in Beijing.

Category	2002	2003	2004	2005	2006	2007	2008	2009	2010	2011	2012	2013	2014	2015	2016	2017
GDP (10^8 yuan)	4396	5104	6164	7141	8312	10071.9	11392	12419	14441.6	16627.9	18350	20330.1	21944.1	23685.7	25669.1	28000.4
Population (10^4)	1423.2	1456.4	1492.7	1538	1601	1676	1771	1860	1961.9	2018.6	2069.3	2144.8	2151.6	2170.5	2172.9	2170.7
Energy consumption (10^4 ton)	4436.1	4648.2	5139.6	5049.8	5399.3	5747.7	5786.2	6008.6	6359.5	6397.3	6564.1	6723.9	6831.2	6852.6	6961.7	7130.6
Vehicular population (10^4)	176.5	212.4	229.6	258.3	287.6	312.8	350.4	398.1	480.9	498.3	520	543.7	559.1	561.9	571.7	590.9
Gasoline ($\times 10^4$ tons)	152	165.22	198.39	235.3	278.16	324.72	340.92	363.61	371.53	389.79	415.9	423.61	440.61	462.76	470.37	489.85
Diesel oil ($\times 10^4$ tons)	109	110.41	131.93	140.86	177.49	192.02	227.22	240.18	237.42	241.12	215.82	193.9	196.46	182.35	172.69	175.11
Coal ($\times 10^4$ tons)	2531	2674	2939	3069	3055.7	2984.7	2747.7	2664.7	2634.6	2365.5	2269.9	2019.23	1736.54	1165.18	847.62	490.46
Natural gas ($\times 10^8$ m^3)	21	21.19	27.02	32.04	40.65	46.64	60.65	69.4	74.79	73.56	92.07	98.81	113.70	145.37	160.30	162.24
Vehicular emission		Euro II			Euro III				Euro IV					Euro V		

937

Atmospheric Chemistry and Physics Discussions

Open Access

938
939
940

Table 3. Mean or median OC and EC mass concentrations observed in the major megacities of the world published in the literature and recorded in this study (in µg/m^3).

Megacities	Method	Period	The number or frequency of samples	OC	EC	literature
Athens	TOT	May 2008 to April 2013	Once everyday	2.1	0.54	Paraskevopoulou et al. 2014
Beijing	TOT	March 2017-Feburary 2018	Hourly	7.7	2.6	This study
Hongkong	TOR	from July to October 2014 and December 2014 to March 2015	N=161	7.8	2.2	Chen et al., 2018
Lhasa	TOR	May 2013 to March 2014	once each week	3.27	2.24	Li et al., 2016
Los Angele	TOT	March 2017-Feburary 2018	once every 3 days	2.88	0.56	US EPA*
Mexico	TOT	March 2006	Hourly	5.4-6.4	0.6-2.1	Yu et al., 2009
Mumbai	TOT	March-May 2007, October-November 2007 and December-January 2007-2008	15 days in a season	20.4-31.3	5.0-9.2	Villalobos et al., 2015
New Delhi	TOR	January 2013 -May 2014	N=95	17.7	10.3	Sharma and Mandal, 2017
New York	TOT	March 2017-Feburary 2018	Once every 3 days	2.88	0.63	US EPA*
Paris	TOT	from 11 September 2009 to 10 September 2010	Once everyday	3.0	1.4	Bressi et al., 2013
São Paulo	TOT	2014	Once each Tuesday	10.2	7	Pereira et al., 2017
Shanghai	TOT	from July 2013 to June 2014	Hourly	8.4	3.1	Xu et al., 2018
Soul	TOT	from January 2014 to December 2014	Hourly	4.1	1.6	Park et al., 2015
Tianjin	TOR	from Dec 23, 2013, to Jan 16, 2014	N=25	30.53	8.21	Wu et al., 2015
Tokyo	TOT	from July 27 to August 15, 2014	Once everyday	2.2	0.6	Miyakawa et al., 2016
Toronto	TOT	December 1, 2010-November 30, 2011	Hourly	3.39	0.5	Sofowote et al., 2014
Wuhan	TOT	From August 2012 to July 2013	Once every six days	16.9	2.0	Zhang et al., 2015
Xi'an	TOR	Four months of 2010	N=56	18.6	6.7	Wang et al., 2015

*https://aqs.epa.gov/api

941

Atmospheric
Chemistry
and Physics
Discussions

Table 4. The ratios of OC/EC in main domestic and foreign cities.

Cities		Period	Method	OC/EC	References
Domestic cities	Beijing	1999-2000	TOR	2.7	He et al., 2001
		2000	TOT	7.0	Song et al., 2006
		2001-2002	EA	2.6	Duan et al., 2006
		2005-2006	TOT	3.0	Yang et al., 2011b
		2008	TOT	2.2	Yang et al., 2011a
		2008-2010	TOR	4.4	Hu et al., 2015
		2009-2010	TOR	2.9	Zhao et al., 2013
		2009-2010	TOT	3.4	Zhang et al., 2013
		2012-2013	TOT	7.0	Wang et al., 2016c
		2013	TOT	5.0	Ji et al., 2018
		2014	TOT	4.8	Ji et al., 2018
		2013	TOT	3.6	This study
		2014	TOT	3.0	This study

942
943

46

Atmospheric
Chemistry
and Physics
Discussions
Open Access
EGU

City	Period	Method	Value	Reference
	2015	TOT	3.0	This study
	2016	TOT	3.0	This study
	2017	TOT	2.9	This study
Baoji	March 2012 - March 2013	TOR	5.3	Niu et al., 2016
Chengdu	2009-2010 annual	TOR	2.5	Tao et al., 2013
	2009–2013	TOR	4.4	Shi et al., 2016
	2011 annual	TOR	2.4	Tao et al., 2014
	2012-2013 annual	TOT	4.1	Chen et al., 2014
Chongqing	2005-2006 annual	TOR	4.7	Yang et al., 2011b
	2012-2013 annual	TOT	3.8	Chen et al., 2014
	May 2012-May 2013	TOT	3.6	Chen Y. et al., 2017
Ya'an	June 2013 - June 2014	TOT	13.3	Li et al., 2018
Hangzhou	2004-2005 annual	EA	2.0	Liu G. et al., 2015
Hongkong	July - October 2014 and December 2014 - March 2015	TOR	3.5	Chen et al., 2018
Lhasa	May 2013 - March 2014	TOR	1.5	Li et al., 2016
Nanjing	2014 annual	TOT	1.8	Chen D. et al., 2017

Atmospheric
Chemistry
and Physics
Discussions

Open Access

EGU

Location	Period	Method	Value	Reference
	2011-2014 annual	TOR	2.6	Li et al., 2015
Ningbo	2009-2010 annual	TOR	2.8	Liu et al., 2013
Neijiang	2012-2013 annual	TOT	4.5	Chen et al., 2014
Qingling	March 2012 - March 2013	TOR	6.3	Niu et al., 2016
	2009 annual	TOR	3.4	Zhao et al., 2015a
	2011	TOT	2.6	Chang et al., 2017
Shanghai	2012	TOT	2.9	Chang et al., 2017
	2012 annual	TOR	5.4	Zhao et al., 2015b
	2013	TOT	3.4	Chang et al., 2017
Shijiazhuang	Four seasons (2009-2010)	TOR	2.7	Zhao et al., 2013
Tianjin	2009-2010	TOR	2.7	Zhao et al., 2013
	2010 annual	TOR	2.7	Wang et al., 2015
	March 2012 - March 2013	TOR	4.0	Niu et al., 2016
Xi'an	March 2012 - March 2013	TOR	4.0	Niu et al., 2016
	March 2012 - March 2013	TOR	3.8	Niu et al., 2016
	December 2014 - November 2015	TOT	10.4	Dai et al., 2018

Atmospheric
Chemistry
and Physics
Discussions

Open Access

	Weinan	March 2012 - March 2013	TOR	4.4	Niu et al., 2016
	Wuhan	From August 2012 - July 2013	TOT	8.5	Zhang et al., 2015
Foreign cities	Athens	May 2008 - April 2013	TOT	3.9	Paraskevopoulou et al. 2014
	Los Angele	March 2017-Feburary 2018	TOT	5.1	US EPA*
	New Delhi	January 2013 -May 2014	TOR	1.7	Sharma and Mandal, 2017
	New York	March 2017-Feburary 2018	TOT	4.6	US EPA*
	Paris	September 11 2009-10 September 2010	TOT	2.1	Bressi et al., 2013
	São Paulo	2014	TOT	1.5	Pereira et al., 2017
	Soul	January 2014 - December 2014	TOT	2.6	Park et al., 2015
	Tokyo	July 27 - August 15, 2014	TOT	3.7	Miyakawa et al., 2016
	Toronto	December 1, 2010-November 30, 2011	TOT	6.8	Sofowote et al., 2014

944 *https://aqs.epa.gov/api